

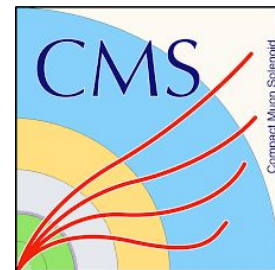
Multiboson measurements



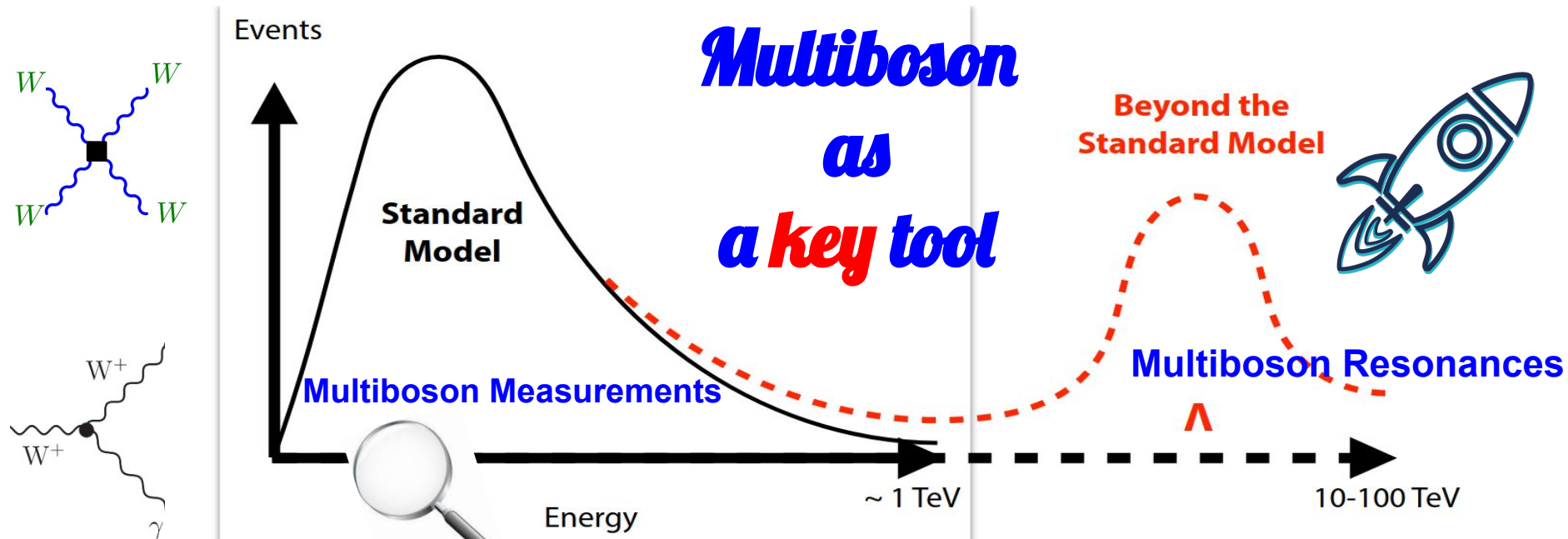
Qiang Li (Peking University)

2023/05/26 LHCP2023

on behalf of the ATLAS & CMS collaborations

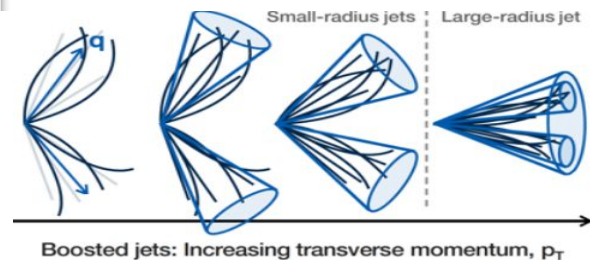


Direct and Indirect Searches for BSM



Anomalous couplings, EFT

$$L_{\text{EFT}} = L_{\text{SM}} + \sum_i \frac{C_i^{(6)}}{\Lambda^2} \mathcal{O}_i^{(6)} + \sum_i \frac{C_i^{(8)}}{\Lambda^4} \mathcal{O}_i^{(8)} + \dots$$



Great Potential to explore unknown

The large boson-boson collider

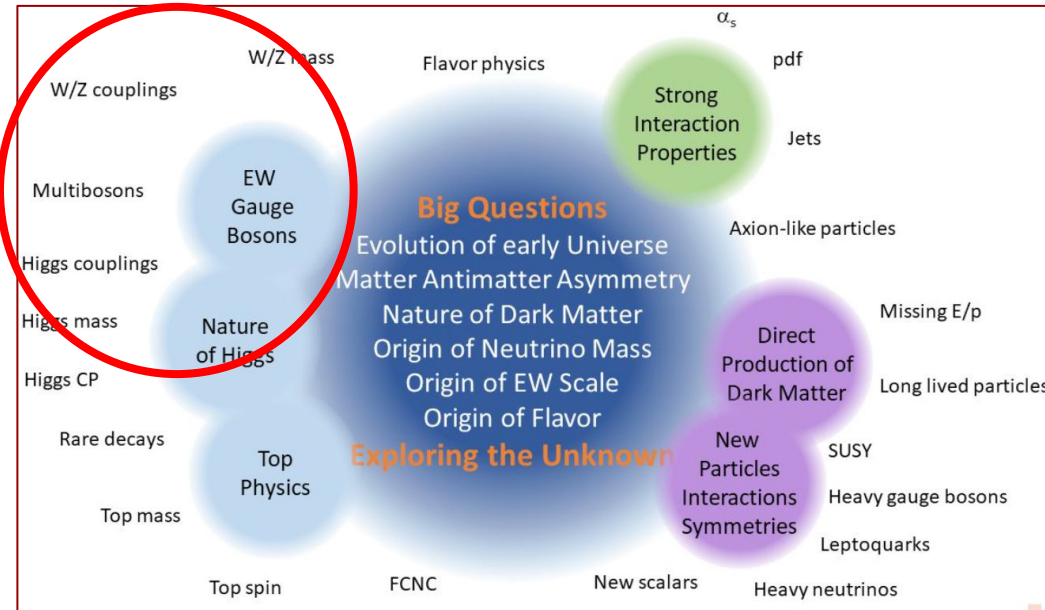
Symmetry

High energy.

High multiplicity.

High opportunities?

[Brian Henning](#)



$$|H|^2 \sim (v + h)^2 + \vec{\phi}^2$$

ops that modify HC will induce processes with longitudinal vectors

$$\text{HC: } |H|^2 \mathcal{O}_{\text{SM}} \supset v h \mathcal{O}_{\text{SM}}$$

$$\text{HwH: } |H|^2 \mathcal{O}_{\text{SM}} \supset \vec{\phi}^2 \mathcal{O}_{\text{SM}}$$

Snowmass 2022

Higgs Couplings
without the Higgs

Rich Results from Multiboson Measurements

Stair to X

VV

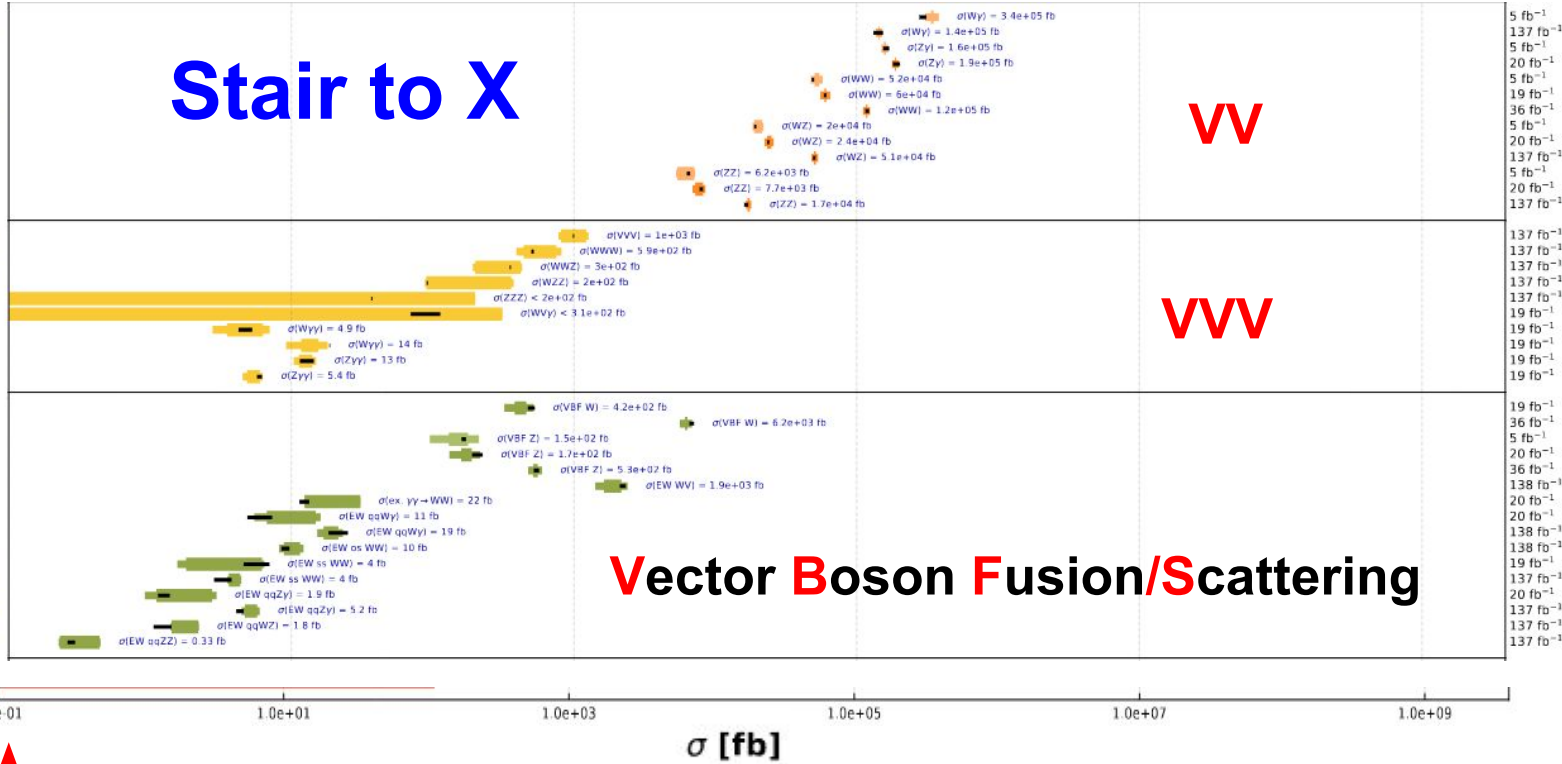
VVV

Vector Boson Fusion/Scattering

Wγ	7 TeV	PRD 89 [2014] 092005
Wγ	13 TeV	PRL 126 252002 [2021]
Zγ	7 TeV	PRD 89 [2014] 092005
Zγ	8 TeV	JHEP 04 (2015) 164
WW	7 TeV	EPJC 73 (2013) 2610
WW	8 TeV	EPJC 75 (2015) 401
WW	13 TeV	PRD 102 092001 [2020]
WZ	7 TeV	EPJC 77 (2017) 236
WZ	8 TeV	EPJC 77 (2017) 236
WZ	13 TeV	Submitted to JHEP
ZZ	7 TeV	JHEP 01 (2013) 063
ZZ	8 TeV	PLB 740 (2015) 250
ZZ	13 TeV	EPJC 81 (2021) 200

VVV	13 TeV	PRL 125 151802 [2020]
WWW	13 TeV	PRL 125 151802 [2020]
WWZ	13 TeV	PRL 125 151802 [2020]
WZZ	13 TeV	PRL 125 151802 [2020]
ZZZ	13 TeV	PRL 125 151802 [2020]
WVγ	8 TeV	PRD 90 032008 [2014]
Wγγ	8 TeV	JHEP 10 (2017) 072
Wγγ	13 TeV	JHEP 10 (2021) 174
Zγγ	8 TeV	JHEP 10 (2017) 072
Zγγ	13 TeV	JHEP 10 (2021) 174

VBF W	8 TeV	JHEP 11 (2016) 147
VBF W	13 TeV	EPJC 80 (2020) 43
VBF Z	7 TeV	JHEP 10 (2013) 101
VBF Z	8 TeV	EPJC 75 (2015) 56
VBF Z	13 TeV	EPJC 78 (2018) 589
EW WW	13 TeV	Submitted to PLB
ex γγ → WW	8 TeV	JHEP 08 (2016) 119
EW qqWγ	8 TeV	JHEP 06 (2017) 106
EW qqWγ	13 TeV	SMP 21-011
EW ss WW	13 TeV	Submitted to PLB
EW ss WW	8 TeV	PRL 114 051801 [2015]
EW ss WW	13 TeV	PRL 120 081801 [2018]
EW qqZγ	8 TeV	PLB 770 (2017) 380
EW qqZγ	13 TeV	PRD 104 072001 [2021]
EW qqWZ	13 TeV	PLB 809 (2020) 135/10
EW qqZZ	13 TeV	PLB 812 (2020) 135992



↑
0.1fb

[CMS](#) SM Summary Plot 2022/9

(see also [ATLAS](#))

Boson Blossom from This Week: *selected results today*

VBS/VBF measurements (with photons) at ATLAS and CMS

Speaker: Ying An (Deutsches Elektronen-Synchrotron (DE))

VBS/VBF theory developments

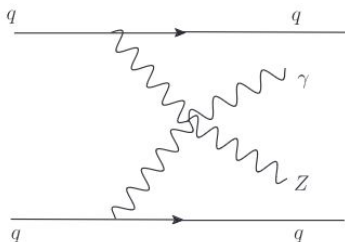
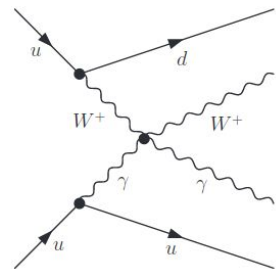
Speakers: Dr Richard Ruiz, Richard Ruiz (University of Pittsburgh)

VBS/VBF measurements (without photons) at ATLAS

Speaker: Chilufya Mwewa (Brookhaven National Laboratory (US))

VBS/VBF measurements (without photons) at CMS

Speaker: Mr Giacomo Boldrini (Universita & INFN, Milano-Bicocca (IT))



Theory prediction and event generation for polarization measurements

Speakers: Giovanni Pelliccioli (Max-Planck-Institut für Physik), Giovanni Pelliccioli (Würzburg University)

Recent diboson and polarization measurements at ATLAS

Speaker: José Antonio Fernández Pretel (Albert Ludwigs Universität Freiburg (DE))

Recent diboson and polarization measurements at CMS

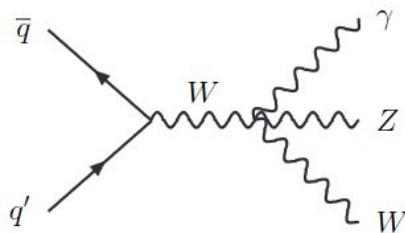
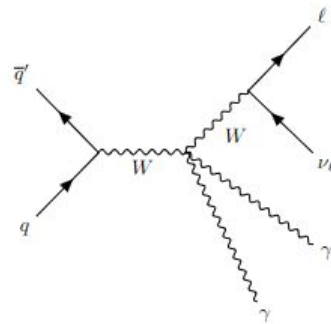
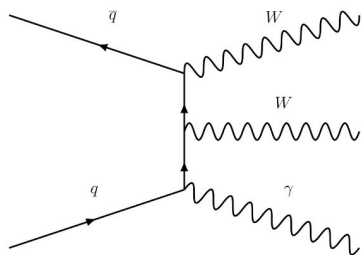
Speaker: Saptaparna Bhattacharya (Northwestern University (US))

Higher-order corrections in multiboson production

Speaker: Silvia Zanoli

Triboson measurements at ATLAS and CMS

Speaker: Alessandro Ambler (McGill University, (CA))



Vector boson modeling for precision physics

Speaker: Tobias Neumann

Recent EWK precision measurements in CMS

Speaker: Vladimir Cherepanov (University of Florida (US))

Recent EWK precision measurements in ATLAS

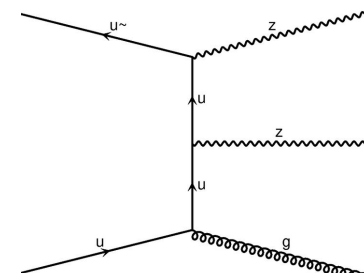
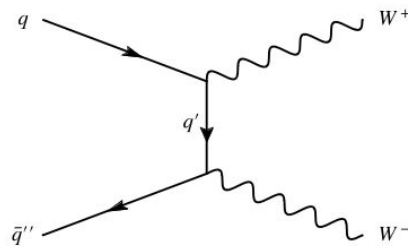
Speaker: Dr Xingguo Li (McGill University, (CA))

Recent EWK precision measurements in LHCb

Speaker: Jianqiao Deng (Central China Normal University CCNU (CN))

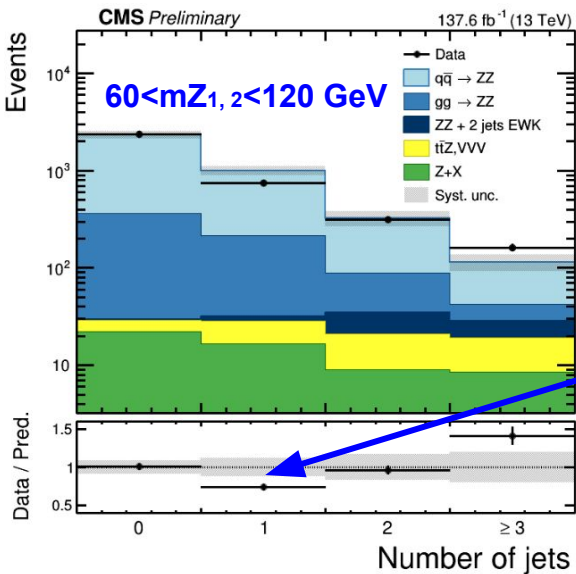
EFT theory outlook

Speaker: Dr Raquel Gomez Ambrosio (Milano Bicocca)



- ZZ production associated with jets in the fully leptonic final states
- Unfolding using the iterative D'Agostini's method including correction for background contributions, with the RooUnfold toolkit.
- **Basic mZ requirement:** $40 < m_{Z_1} < 120$ GeV, $4 < m_{Z_2} < 120$ GeV
 - **On-shell requirement:** $60 < m_{Z_1}, m_{Z_2} < 120$ GeV

Systematic source	Normalized
Trigger	-
Electron Efficiency	0.13 - 0.3 %
Muon Efficiency	0.02 - 0.08 %
Jet energy resolution	1.65 - 3.85 %
JES correction	0.93 - 5.32 %
Reducible background	0.05 - 0.43 %
Pileup	0.04 - 1.08 %
Luminosity	< 0.03 %
Monte Carlo choice	0.52 - 4.52 %
gg cross section	0.01 - 0.19 %
QCD Scales	0.16 - 0.82 %
PDF	0.05 - 0.12 %
α_s	0.01 - 0.1 %



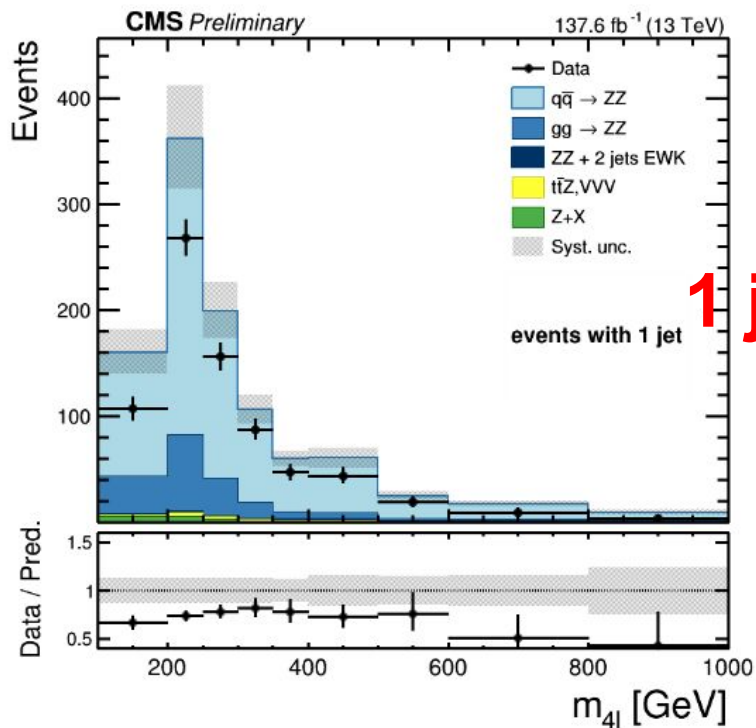
Data in the 0 and 2 jet bins are well described by the predictions,

Significant discrepancy **In the 1 jet bin,**

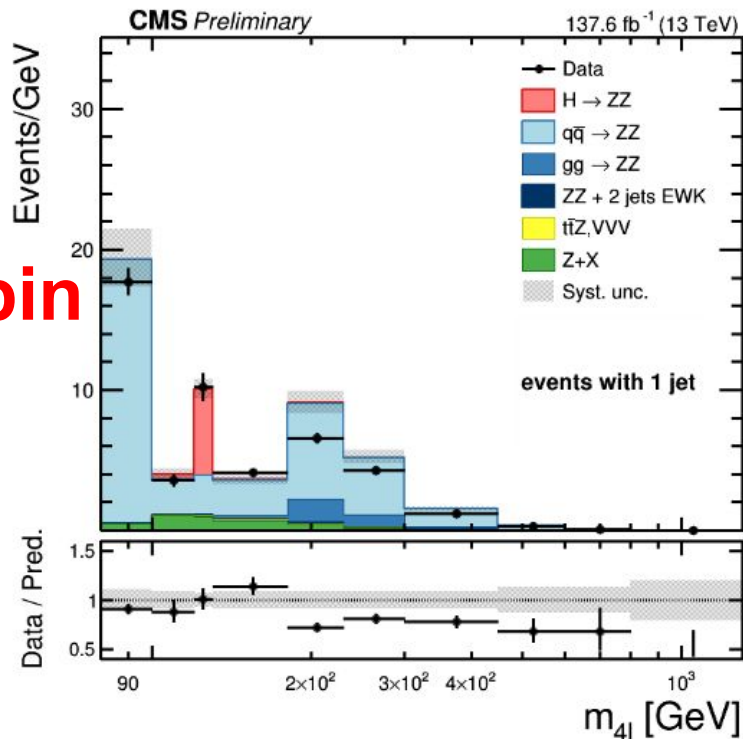
The description of events with ≥ 3 jets requires NNLO and even higher order corrections, thus **the discrepancy at high jets bin is expected.**

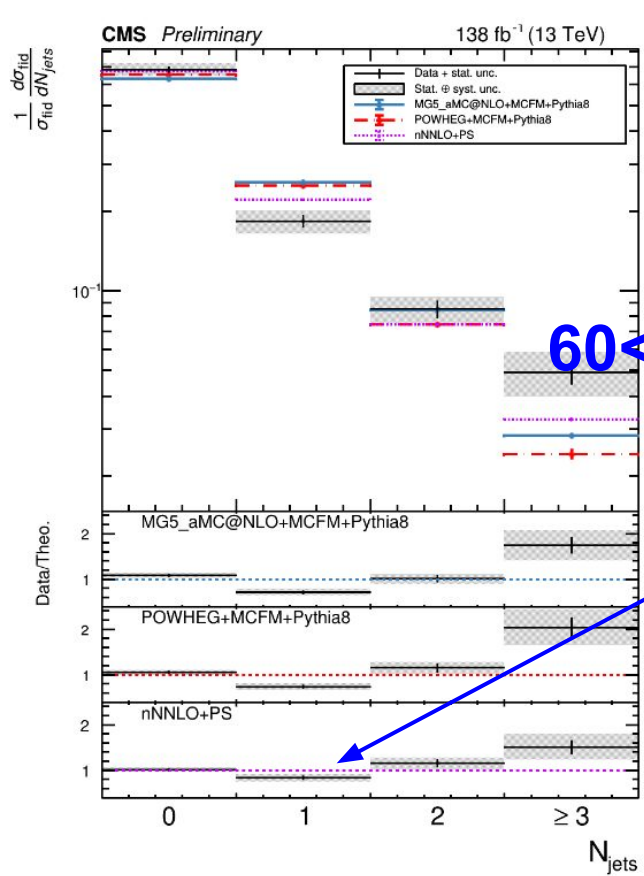
MadGraph ZZ+0/1jet@NLO FxFx, and Powheg ZZ NLO

$60 < m_{Z_{1,2}} < 120$ GeV

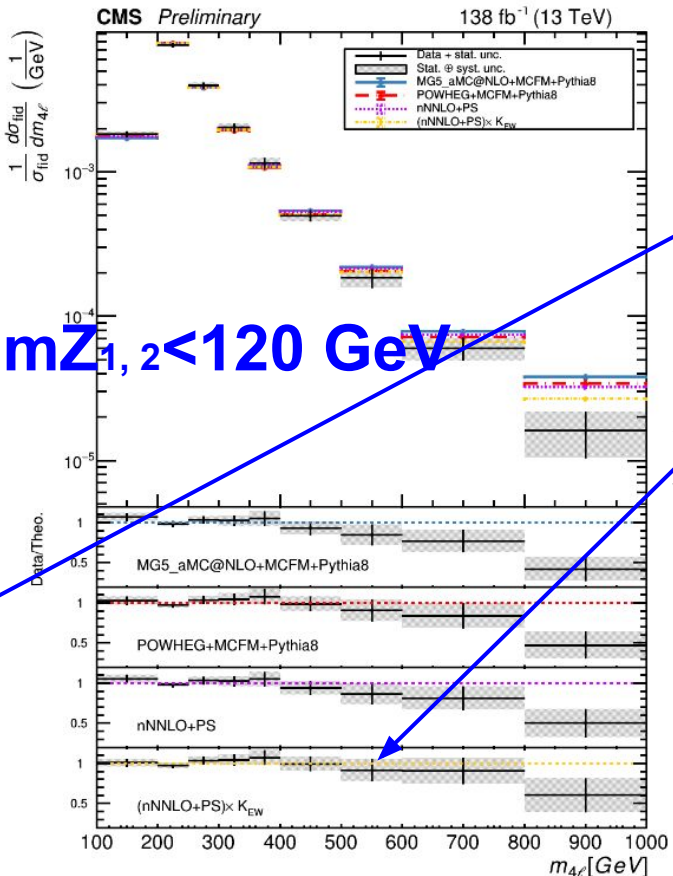


$40 < m_{Z_1} < 120$ GeV $4 < m_{Z_2} < 120$ GeV





60 < m_{Z_{1,2}} < 120 GeV



In general, the **nNNLO+PS** prediction describes the **N_{jet}** distribution better.

The **EW corrected nNNLO+PS** predictions describe the measured values better than those without the EW corrections

The **EW corrections** have negligible effect on any other normalized distributions than **m_{4l}**.

1D and 2D differential distributions data-driven backgrounds

Z+Jets, Pile-up, tt γ

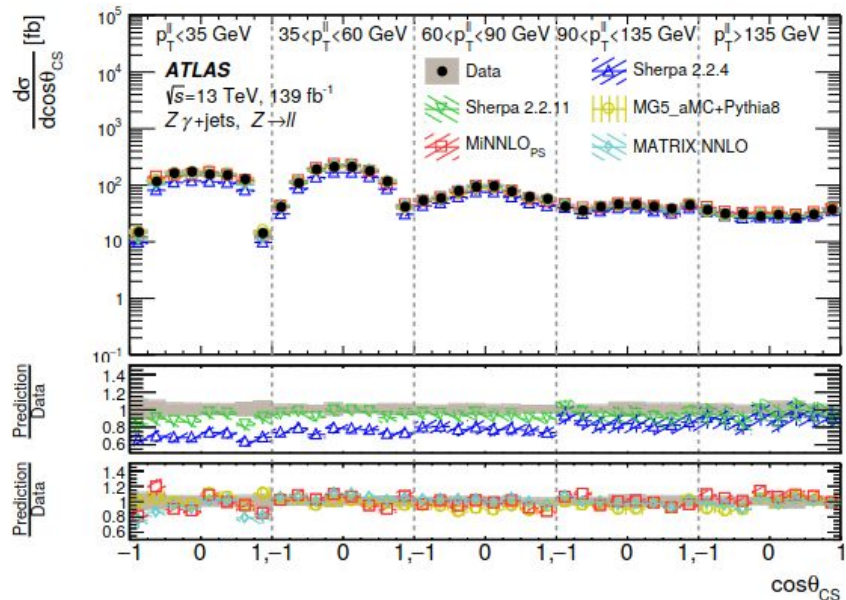
Uncertainties 4-10%

Jet energy scale, Bkg modelling

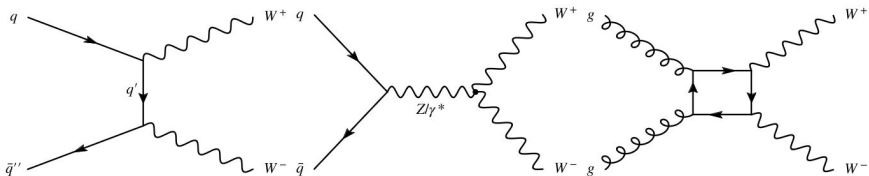
Data general well described

NLO 0,1p in Sherpa improves
description wrt ME+PS @LO

- ◆ $N_{\text{jet}}, p_{T^1}, p_{T^2}, p_{T^1}/p_{T^2}, HT, p_T(\gamma)$ and $p_{T^{\parallel}}/\sqrt{HT}$
 $m_{\parallel\gamma}, m_{jj}, \Delta R(l\ell), \Delta\phi(j, \gamma)$
- ◆ QCD sensitive 2D observables:
 - ◆ $P_{T^{\parallel\gamma}}/m^{\parallel\gamma}$ in bins of $m^{\parallel\gamma}$,
 - ◆ $P_{T^{\parallel}} - P_{T^{\gamma}}$ in bins of $P_{T^{\parallel}} + P_{T^{\gamma}}$,
 - ◆ $P_{T^{\parallel\gamma}}$ in bins of $P_{T^{\parallel}}$
- ◆ Polarisation-sensitive 2D observables:
 - ◆ $\cos\theta_{CS}$ and ϕ_{CS} in bins of $P_{T^{\parallel}}$



Process	Generator	Order	PDF set	PS/UE/MPI
Z γ +jets	SHERPA 2.2.11	0,1j@NLO + 2,3,4j@LO	NNPDF3.0NNLO	SHERPA 2.2.11
Z γ +jets	SHERPA 2.2.4	0,1,2,3j@LO	NNPDF3.0NNLO	SHERPA 2.2.4
Z γ +jets	MADGRAPH5_AMC@NLO	0,1j@NLO	NNPDF3.0NLO_as_0118	PYTHIA 8.212
Purely EW Z γ jj	MADGRAPH5_AMC@NLO	LO	NNPDF3.0LO	PYTHIA 8.240
Z + jets	POWHEG BOX	0j@NLO	CT10NLO	PYTHIA 8.186
tt $\gamma, tW\gamma$	MADGRAPH5_AMC@NLO	LO	NNPDF2.3LO	PYTHIA 8.212
ZZ \rightarrow llll, W $^{\pm}$ Z \rightarrow lllv	SHERPA 2.2.2	0,1j@NLO + 2,3j@LO	NNPDF3.0NNLO	SHERPA 2.2.2
WZ $\gamma, WW\gamma$	SHERPA 2.2.11	0j@NLO + 1,2j@LO	NNPDF3.0NNLO	SHERPA 2.2.11



Lepton selection	1 electron and 1 muon of opposite charge, no additional lepton with $p_T > 10$ GeV, Loose isolation, and LooseLH (electron) / Loose (muon) identification
Number of b -jets	0
Dilepton invariant mass	> 85 GeV

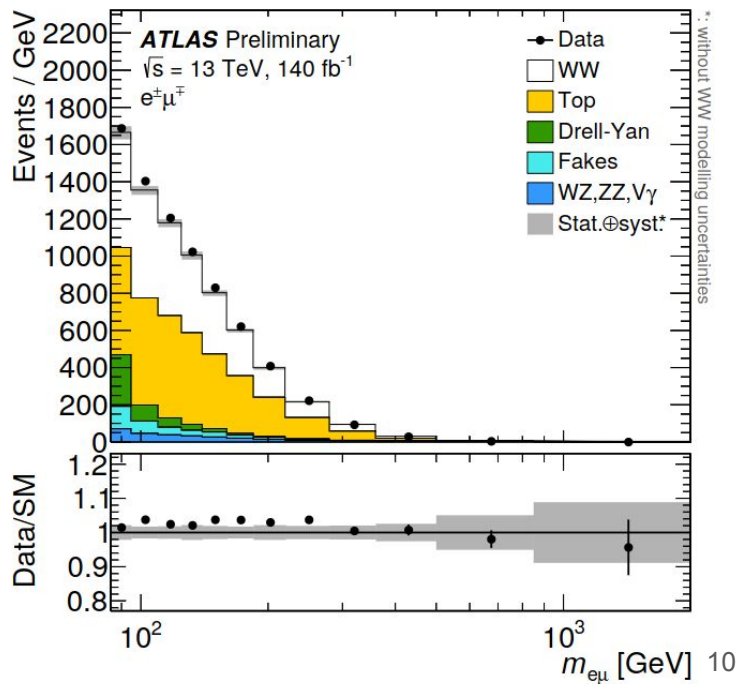
- **Jet-inclusive $WW \rightarrow e\mu$ Measurements**
- **Dominant bkg from top-related processes**
b-tag counting method

$$N_{2b}^{t\bar{t}} = N_{\geq 0b}^{t\bar{t}} \cdot C_b \varepsilon_b^2,$$

$$N_{1b}^{t\bar{t}} = N_{\geq 0b}^{t\bar{t}} \cdot (2\varepsilon_b - C_b \varepsilon_b^2),$$

$$N_{0b}^{t\bar{t}} = N_{\geq 0b}^{t\bar{t}} \cdot (1 - 2\varepsilon_b + C_b \varepsilon_b^2)$$

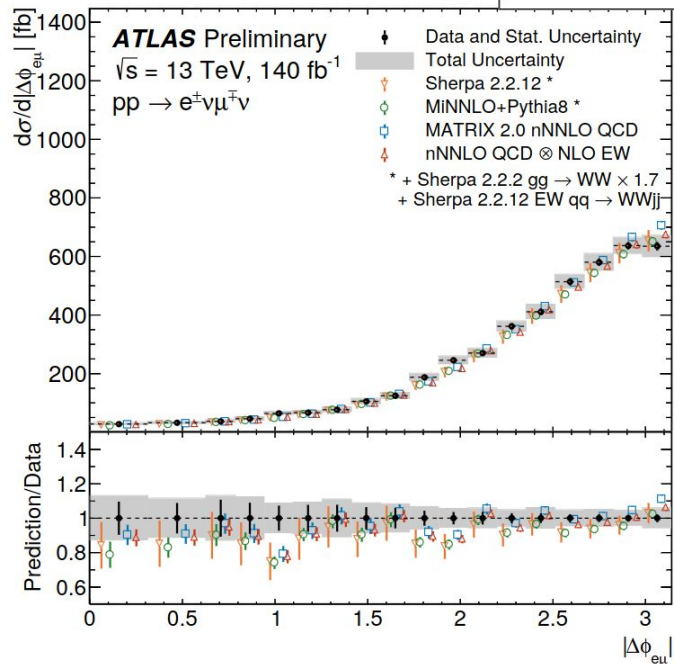
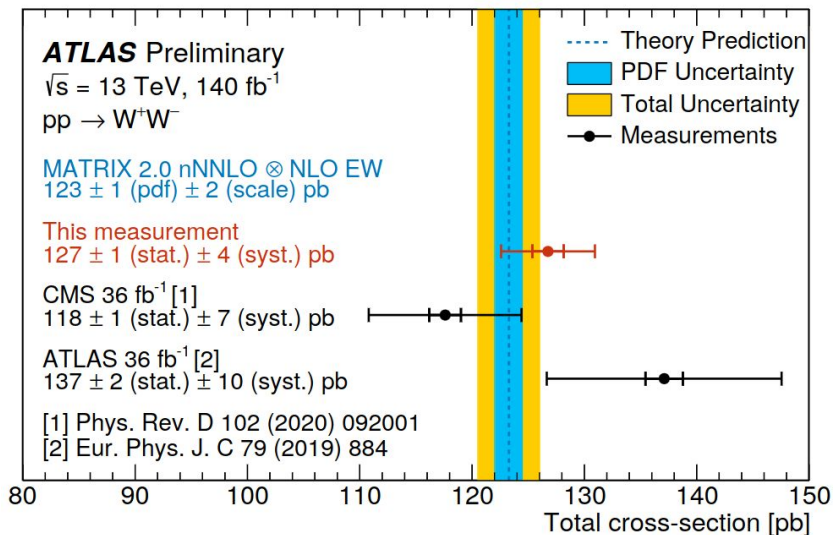
Process	Generator	Parton shower	Matrix element $O(\alpha_S)$	Normalization
$q\bar{q} \rightarrow WW$	MinNLO	PYTHIA8	NNLO	Generator
$gg \rightarrow WW$	SHERPA2.2.2	SHERPA	LO (0–1 jet)	NLO
$t\bar{t}$	POWHEG BoxV2	PYTHIA8	NLO	NNLO+NNLL
Wt	POWHEG BoxV2	PYTHIA8	NLO	NLO+NNLL
Z+jets	SHERPA2.2.1	SHERPA	NLO (0–2 jets), LO (3–4 jets)	NNLO
WZ, ZZ	SHERPA2.2.2	SHERPA	NLO (0–1 jet), LO (2–3 jets)	Generator [†]
$W\gamma, Z\gamma$	SHERPA2.2.8	SHERPA	NLO (0–1 jet), LO (2–3 jets)	Generator [†]



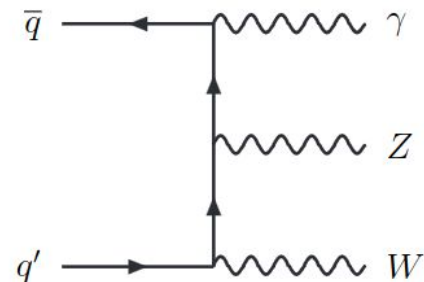
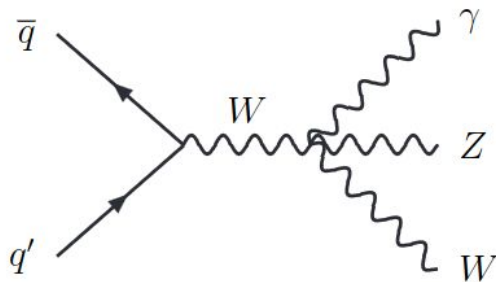
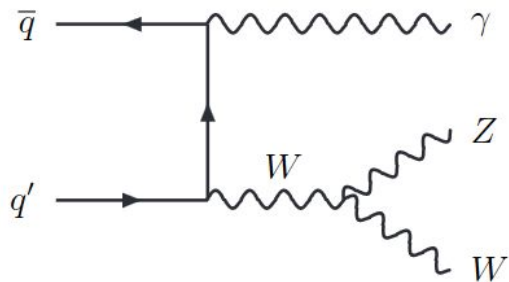
* without WW modelling uncertainties

Uncertainty source	Effect
Total uncertainty	3.1%
Stat. uncertainty	1.1%
Top modelling	1.6%
Fake lepton background	1.5%
Flavour tagging	0.7%
Other background	0.9%
Signal modelling	1.0%
Jet calibration	0.6%
Luminosity	0.8%
Other systematic uncertainties	0.9%

- The measured fiducial XS for WW production with $WW \rightarrow e\mu$ is $707 \pm 7(stat.) \pm 20(syst.) fb$
- The measurements is extrapolated to the full phase space of WW production $127 \pm 1(stat.) \pm 4(syst.) pb$



WZ γ observation ATLAS-CONF-2023-014



- **Pure leptonic final state,**
- **Signal modelled by Sherpa 2.2.11**
0@NLO QCD+1,2@LO QCD
Merged with Parton shower
- **FSR photon suppressed:**
 $m_{ll} > 81 \text{ GeV}$ (of the Z-lepton pair)
- **main backgrounds:**
Non-prompt photons or leptons
- **WZ γ , ZZ γ and ZZ fitted simultaneously**

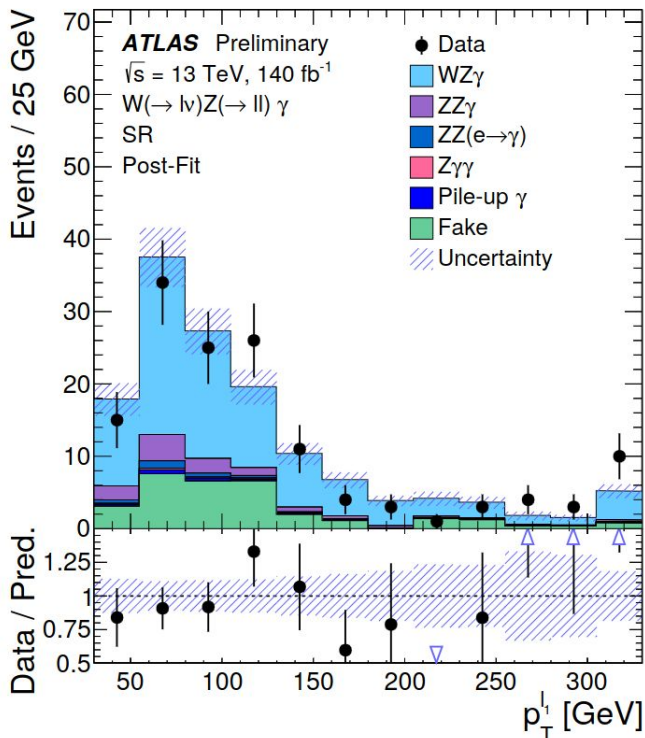
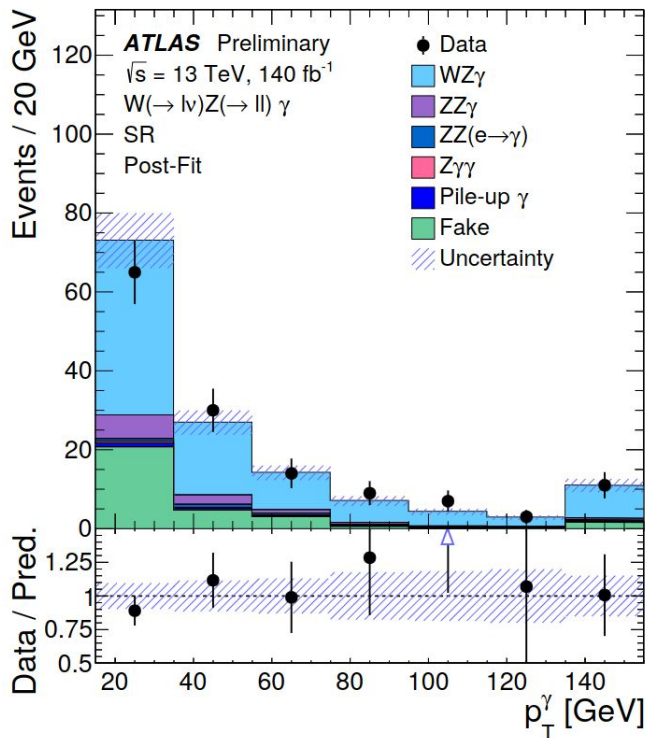
Process	SR	ZZ γ CR	ZZ($e \rightarrow \gamma$) CR
WZ γ	92 \pm 15	0.21 \pm 0.07	0.56 \pm 0.14
ZZ γ	10.7 \pm 2.3	23 \pm 5	1.8 \pm 0.4
ZZ($e \rightarrow \gamma$)	3.0 \pm 0.6	0.028 \pm 0.020	30 \pm 6
Z $\gamma\gamma$	1.05 \pm 0.32	0.15 \pm 0.06	0.29 \pm 0.10
Non-prompt background	30 \pm 6	-	-
Pile-up γ	1.9 \pm 0.7	-	-
Total prediction	139 \pm 12	23 \pm 5	33 \pm 6
Data	139	23	33

WZ γ observation *ATLAS-CONF-2023-014*

$(e\mu\mu, \mu ee, eee, \mu\mu\mu)$ channels combined
profile-likelihood fit in SR+2CRs

6.3 (5.0) σ obs.(exp.)

$$\sigma_{WZ\gamma} = 2.01 \pm 0.30 \text{ (stat.)} \pm 0.16 \text{ (syst.) fb,}$$

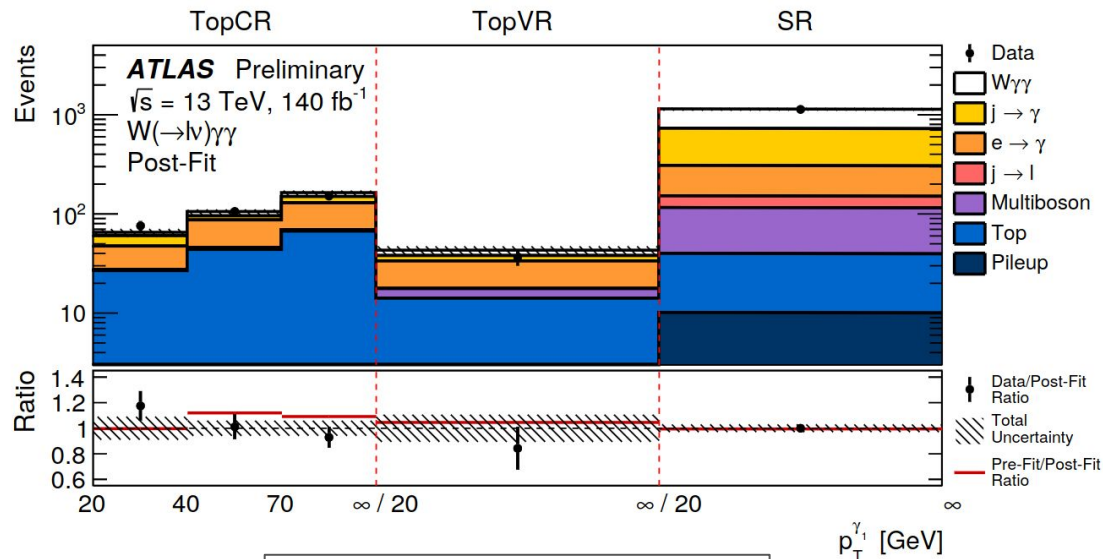


W $\gamma\gamma$ observation ATLAS-CONF-2023-005

- Dominant background from non-prompt leptons and photons
- Main source of systematics due to data-driven bkg estimates

5.6 (5.6) σ obs.(exp.)

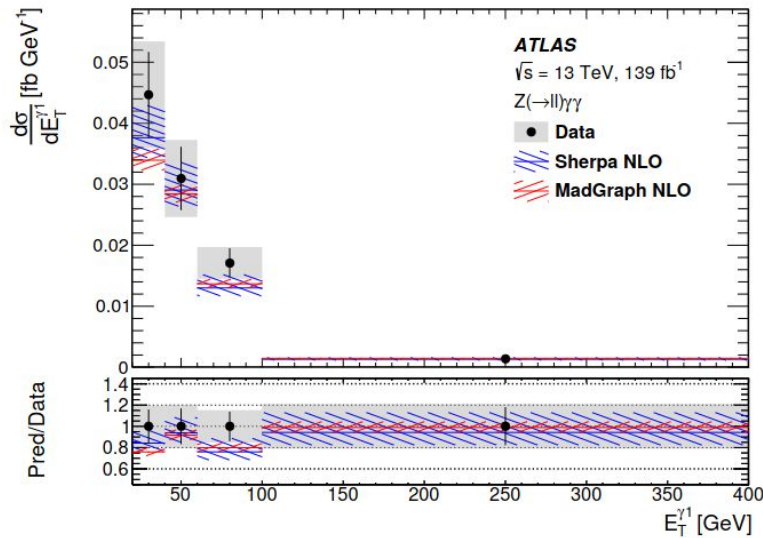
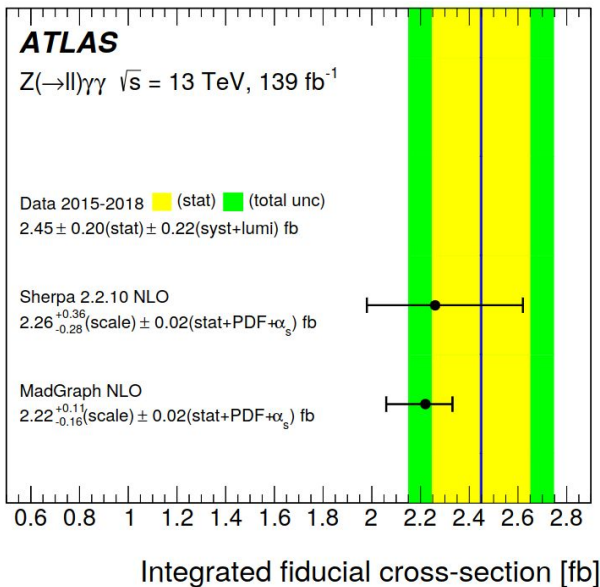
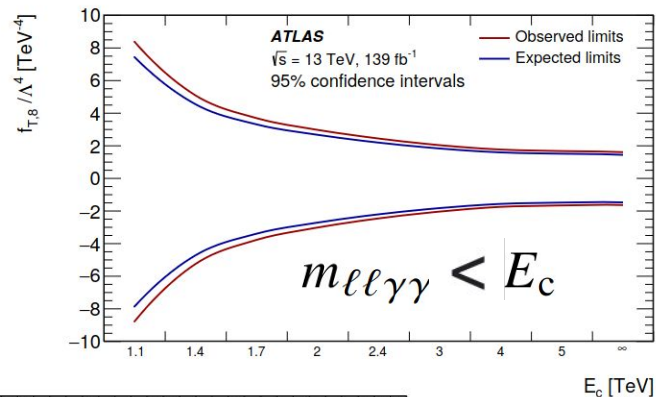
Source of uncertainty	Impact [%]
Data-driven background estimates	13
Photon efficiency	4.5
Signal MC theoretical modeling	3.5
Background MC theoretical modeling	3.0
Monte Carlo statistics	2.8
Jet efficiency and calibration	2.4
Top normalization	2.4
Pileup reweighting	1.6
E_T^{miss} calibration	1.4
Muon efficiency and calibration	1.4
Luminosity	1.0
Electron and photon calibration	0.7
Flavor tagging efficiency	0.6
Systematic	15
Statistical	8.3
Total	17



$$\mu_{\text{obs}} = 1.01^{+0.17}_{-0.16}$$

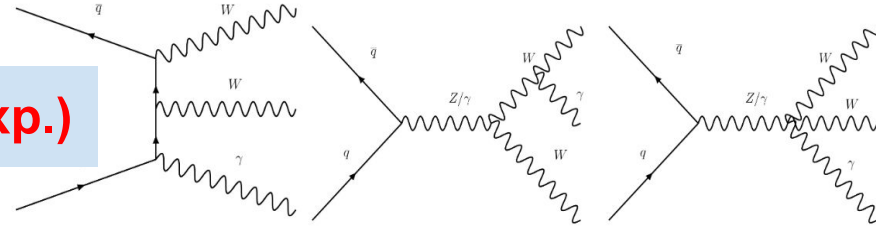
$$\sigma_{\text{obs}}^{\text{fid}} = 12.2^{+2.1}_{-2.0} \text{ fb}$$

- Final-state radiation suppressed by the event selection
- Dominant background from non-prompt photons
- Statistically dominated
 - main syst. from non-prompt photons
- Unfolded differential distributions
- Limited on aQGC with (non-)unitarised treatment

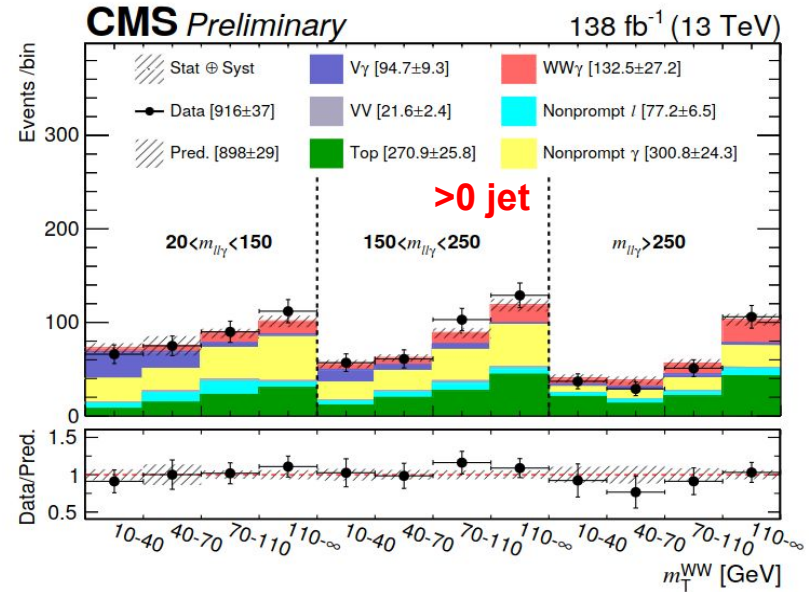
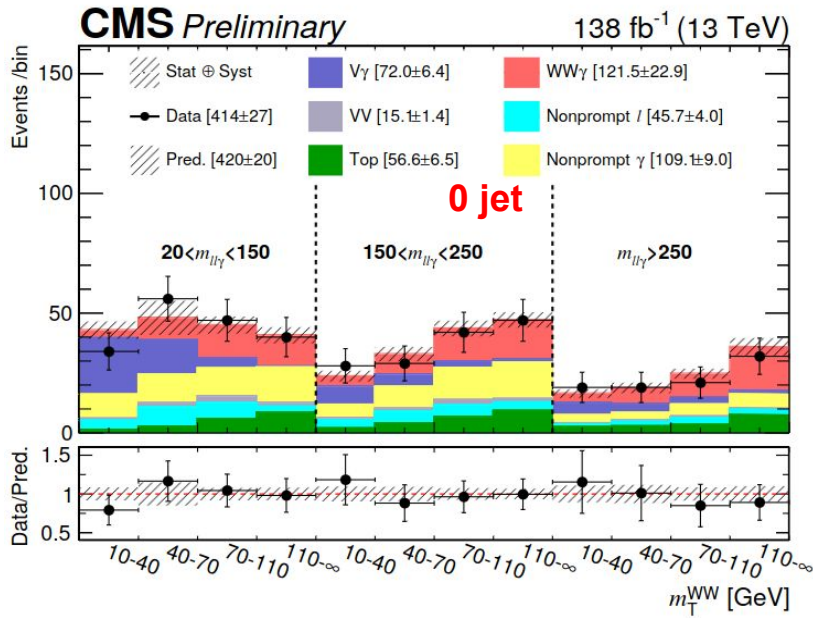


WW γ observation CMS-PAS-SMP-22-006

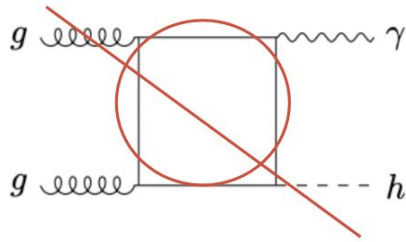
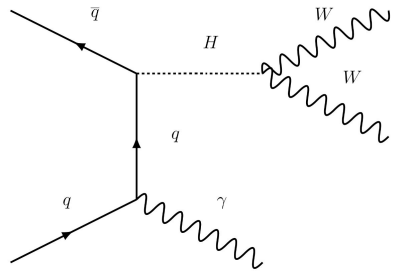
- Signal region categorized with **0 and >0 jet**,
- only **$e\mu$ channel**
- SSWW γ and TOP γ **CRs**, **5.6 (4.7) σ obs.(exp.)**
- data-driven **non-prompt** backgrounds
- maximum likelihood fit of **2D binned distributions**.



$$\mu_{\text{combined}}^{\text{obs.}} = 1.31 \pm 0.17 \text{ (stat)} \pm 0.21 \text{ (syst)}$$

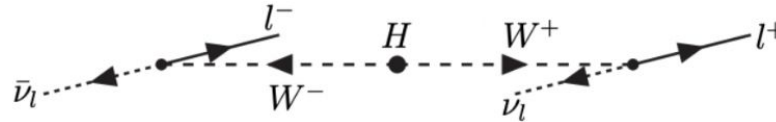


WW γ observation CMS-PAS-SMP-22-006



- Also sensitive to **Higgs couplings with light quarks**
 - no gluon fusion contribution due to Furry's theorem
- **Further optimization targeting the Higgs characteristics**

$$\Delta\phi_{\ell\ell} < 2.5, \Delta R_{\ell\ell} < 2.3, \text{ and } \Delta R_{\ell\gamma} > 0.8$$



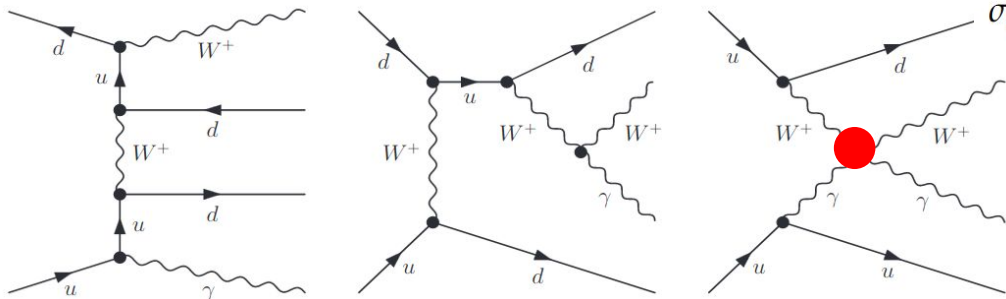
- **H Signal generated with MadGraph at LO**
 - [Higgs effective Lagrangian](#) for u, d and s;
 - Running mass effect included for c

Process	σ_{up} pb exp.(obs.)	Yukawa couplings limits exp.(obs.)
$u\bar{u} \rightarrow H + \gamma \rightarrow e\mu\gamma$	0.067 (0.085)	$ \kappa_u \leq 13000$ (16000)
$d\bar{d} \rightarrow H + \gamma \rightarrow e\mu\gamma$	0.058 (0.072)	$ \kappa_d \leq 14000$ (17000)
$s\bar{s} \rightarrow H + \gamma \rightarrow e\mu\gamma$	0.049 (0.068)	$ \kappa_s \leq 1300$ (1700)
$c\bar{c} \rightarrow H + \gamma \rightarrow e\mu\gamma$	0.067 (0.087)	$ \kappa_c \leq 110$ (200)

VBS $W\gamma$

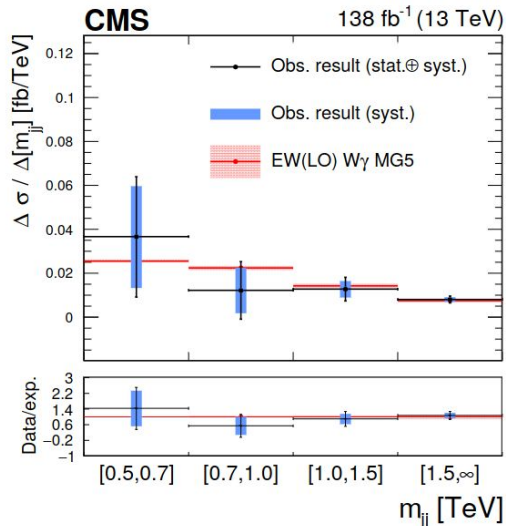
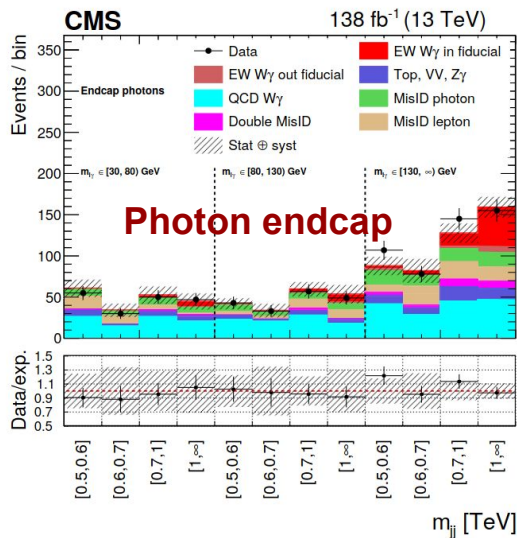
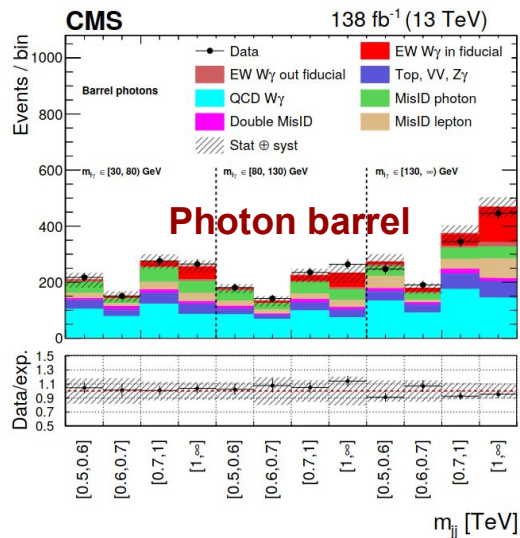
arXiv:2212.12592

accepted by PRD



$$\sigma_{EW}^{\text{fid}} = 23.5 \pm 2.8 \text{ (stat)}_{-1.7}^{+1.9} \text{ (theo)}_{-3.4}^{+3.5} \text{ (syst)} \text{ fb} = 23.5_{-4.7}^{+4.9} \text{ fb.}$$

6.0 (6.8) σ observed (expected)



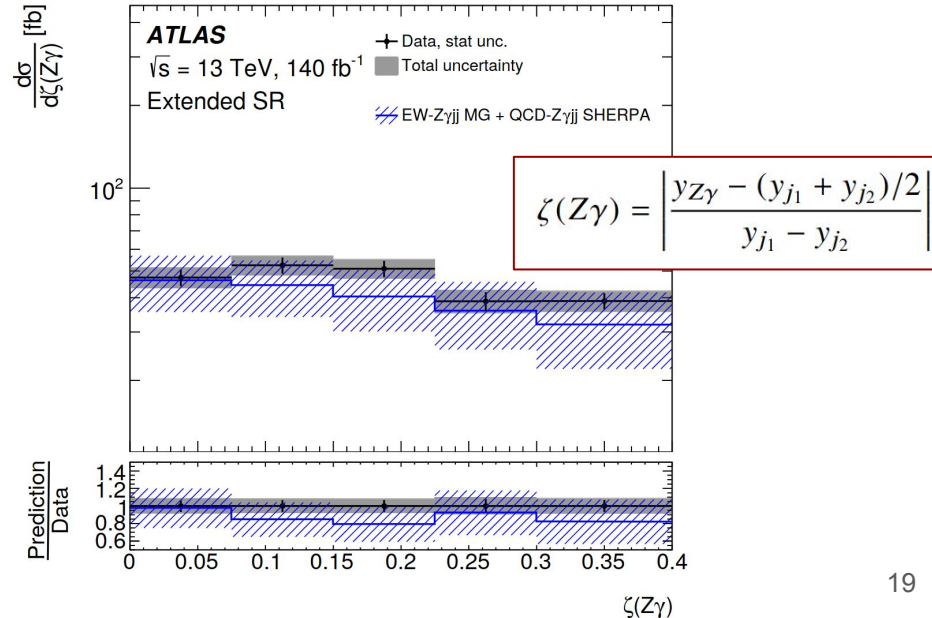
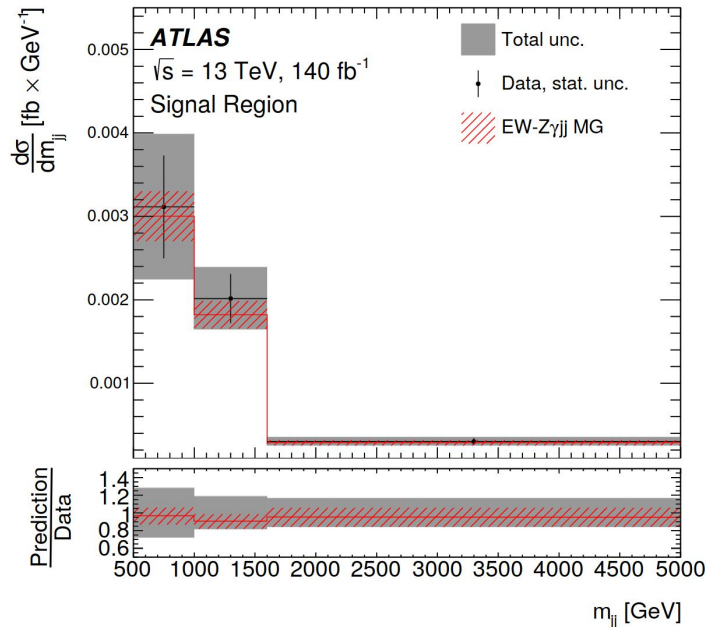
- **Fiducial and differential cross sections;**
- **Stringent limits on aQGCs: fM,2-4 and fT6-7**

Electroweak production of Z γ (Z \rightarrow ee, $\mu\mu$) in association with two jets, Fiducial and differential cross-sections, for both EW and EW+QCD.

$$\mu_{EW} = 1.02 \pm 0.09 \text{ (stat)} \pm 0.09 \text{ (syst)}$$

$$= 1.02^{+0.13}_{-0.12}$$

	Data stat.	MC stat.	Background	Reco	EW mod.	QCD mod.	Total
$\Delta\sigma_{EW}/\sigma_{EW}$ [%]	± 9	± 1	± 1	± 4	$+8$ -6	± 2	± 13
$\Delta\sigma_{Z\gamma}/\sigma_{Z\gamma}$ [%]	± 3	± 1	± 2	-3 $+7$ -6		± 9	$+12$ -11



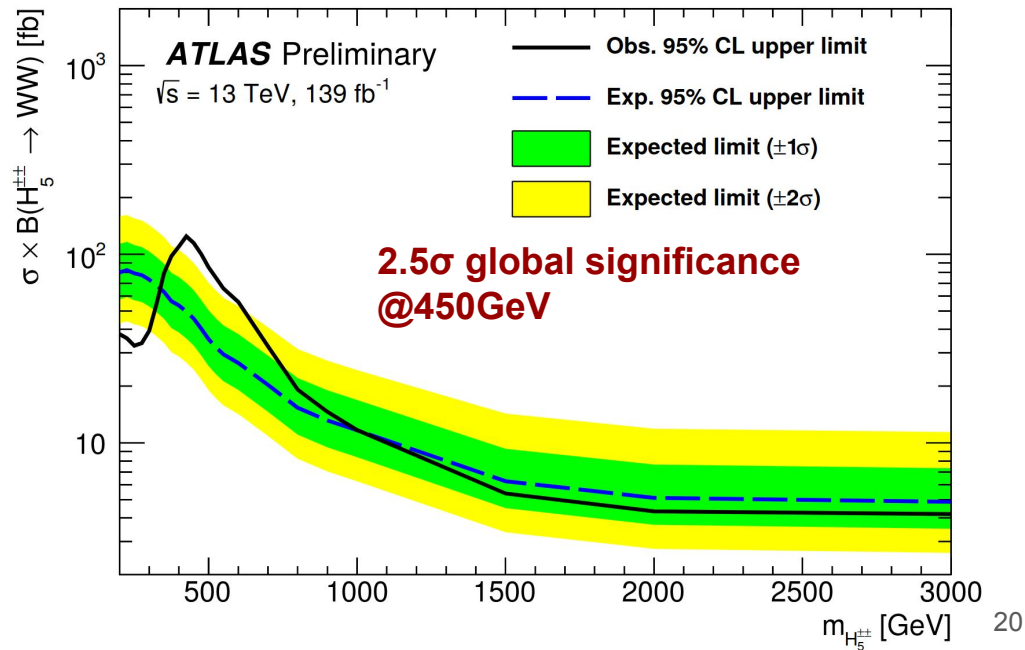
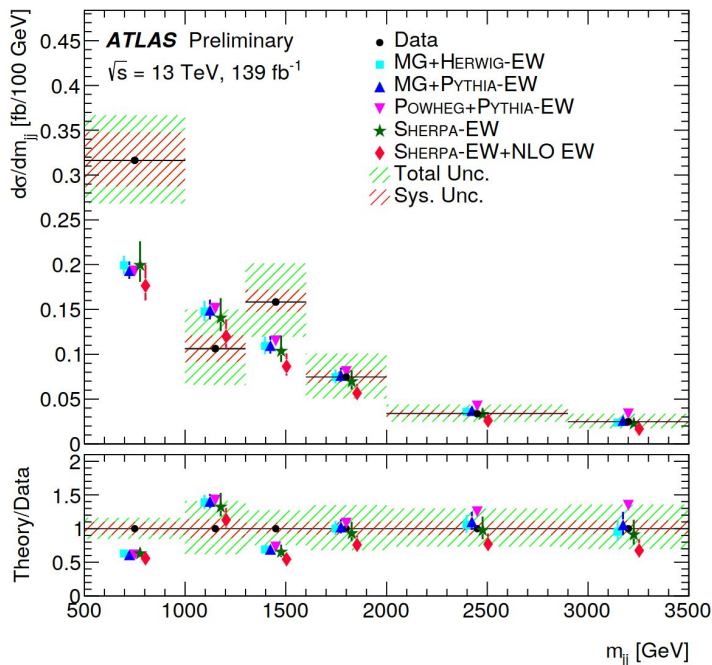
Same-Sign WW

ATLAS-CONF-2023-023



- Fiducial and differential cross sections
- Searches for aQGC, doubly charged Higgs

Description	$\sigma_{\text{fid}}^{\text{EW}}$, fb	$\sigma_{\text{fid}}^{\text{EW+Int+QCD}}$, fb
Measured cross section	2.88 ± 0.21 (stat.) ± 0.19 (syst.)	3.35 ± 0.22 (stat.) ± 0.20 (syst.)
MG_AMC@NLO+HERWIG	2.53 ± 0.04 (PDF) $\pm_{0.19}^{0.22}$ (scale)	2.93 ± 0.05 (PDF) $\pm_{0.27}^{0.34}$ (scale)
MG_AMC@NLO+PYTHIA	2.55 ± 0.04 (PDF) $\pm_{0.19}^{0.22}$ (scale)	2.94 ± 0.05 (PDF) $\pm_{0.27}^{0.33}$ (scale)
SHERPA	2.44 ± 0.03 (PDF) $\pm_{0.27}^{0.40}$ (scale)	2.80 ± 0.03 (PDF) $\pm_{0.36}^{0.53}$ (scale)
POWHEG BOX +PYTHIA	2.67	-

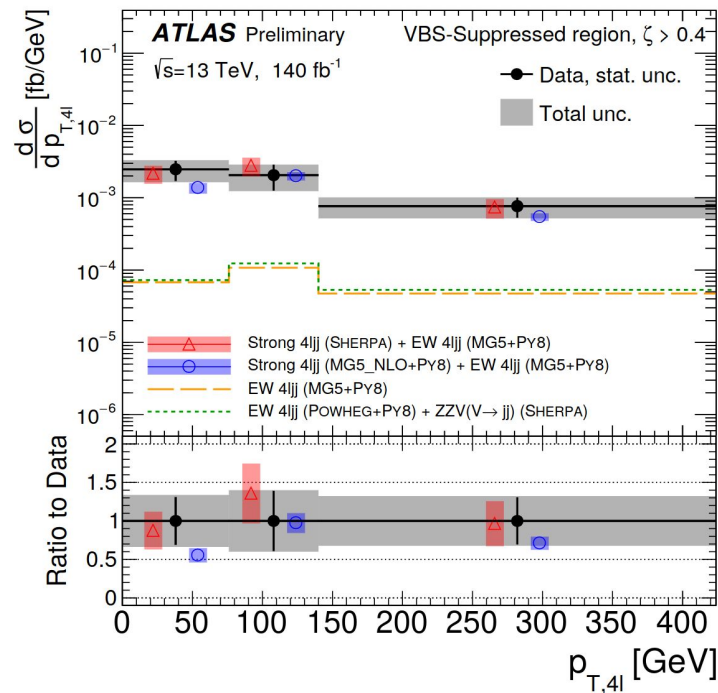
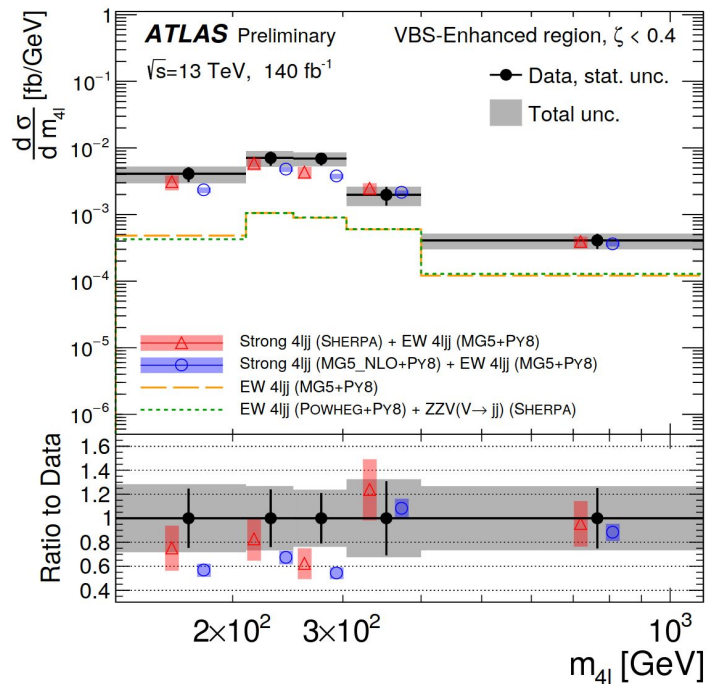
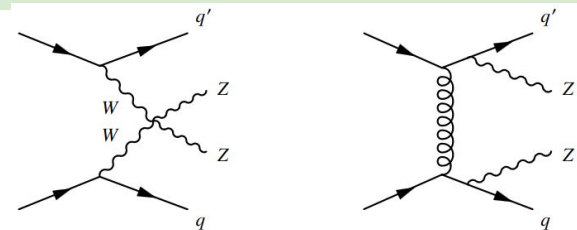


$ZZ \rightarrow 4l + jets$

ATLAS-CONF-2023-024



- Differential cross-section for both EW and Inclusive productions
- Searches for dim-6 and dim-8 EFTs



Summary and Outlook

- **Rich progress and potential from Multiboson Measurements/Probes**
 - Precise measurements on diboson+jets: $ZZ, Z\gamma$
 - First observations of several tri-boson processes: $WZ\gamma, WW\gamma, W\gamma\gamma, Z\gamma\gamma$
 - *Precise VBS measurements: $W/Z\gamma, SSWW, ZZ$*
 - Anomalous coupling, EFT, and even Higgs properties!
- **High energy, High Luminosity, High multiplicity, High opportunities!**
- **Run-3 data accumulating: Keep tuned! More surprise (un)expected.**



Headline News 2030?

LIVE

- Forward and high momentum jets
- Low central jet activity

Jet 2, $p_T = 52.5$ GeV
Jet 1, $p_T = 154.0$ GeV
Muon 2, $p_T = 35.0$ GeV

BREAKING NEWS

R. Sekhar Chivukula

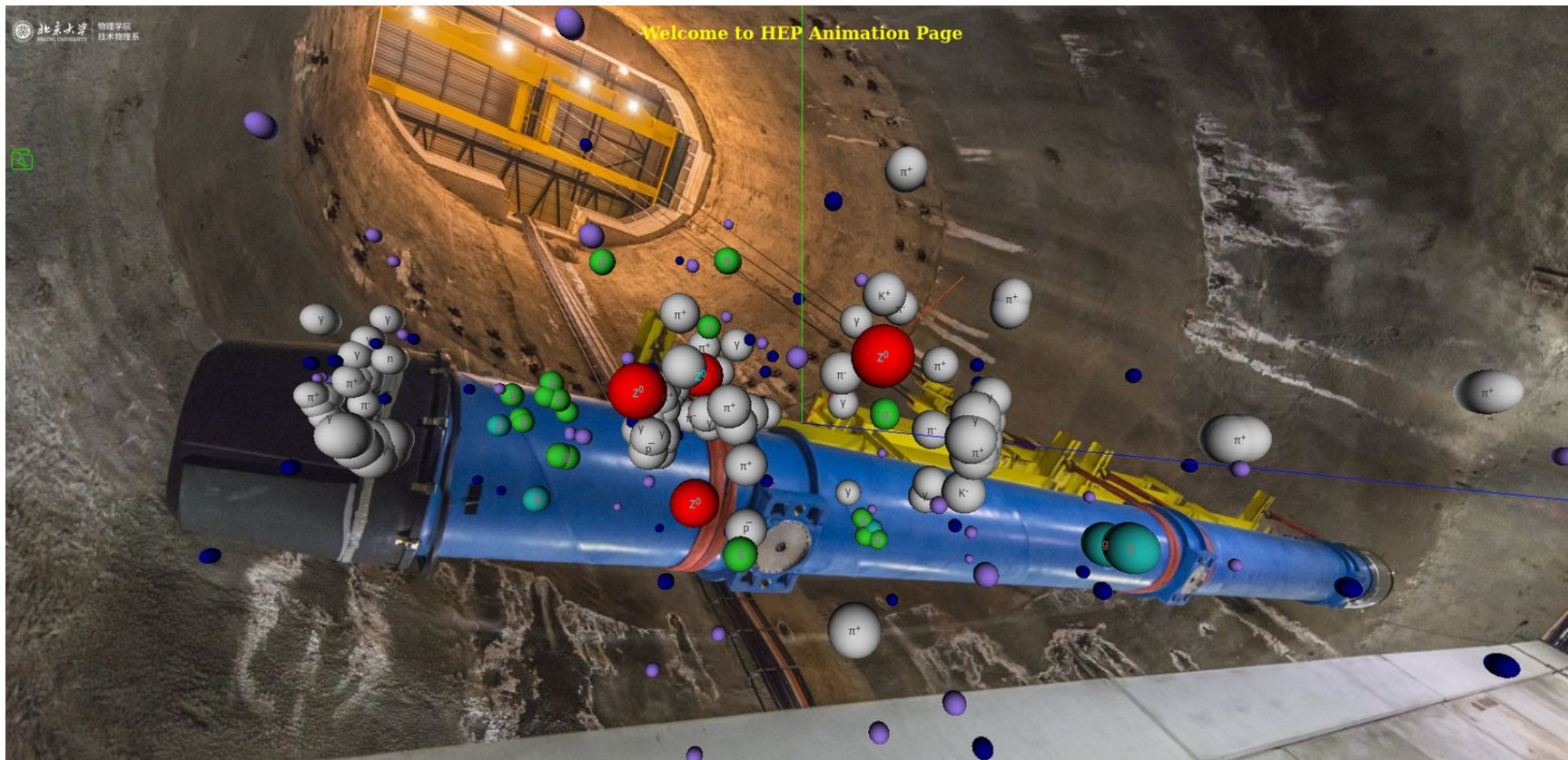
HIGGS UNITARIZES WW SCATTERING

16:11 HL-LHC DELIVERS ON PROMISE TO PROBE EWS!

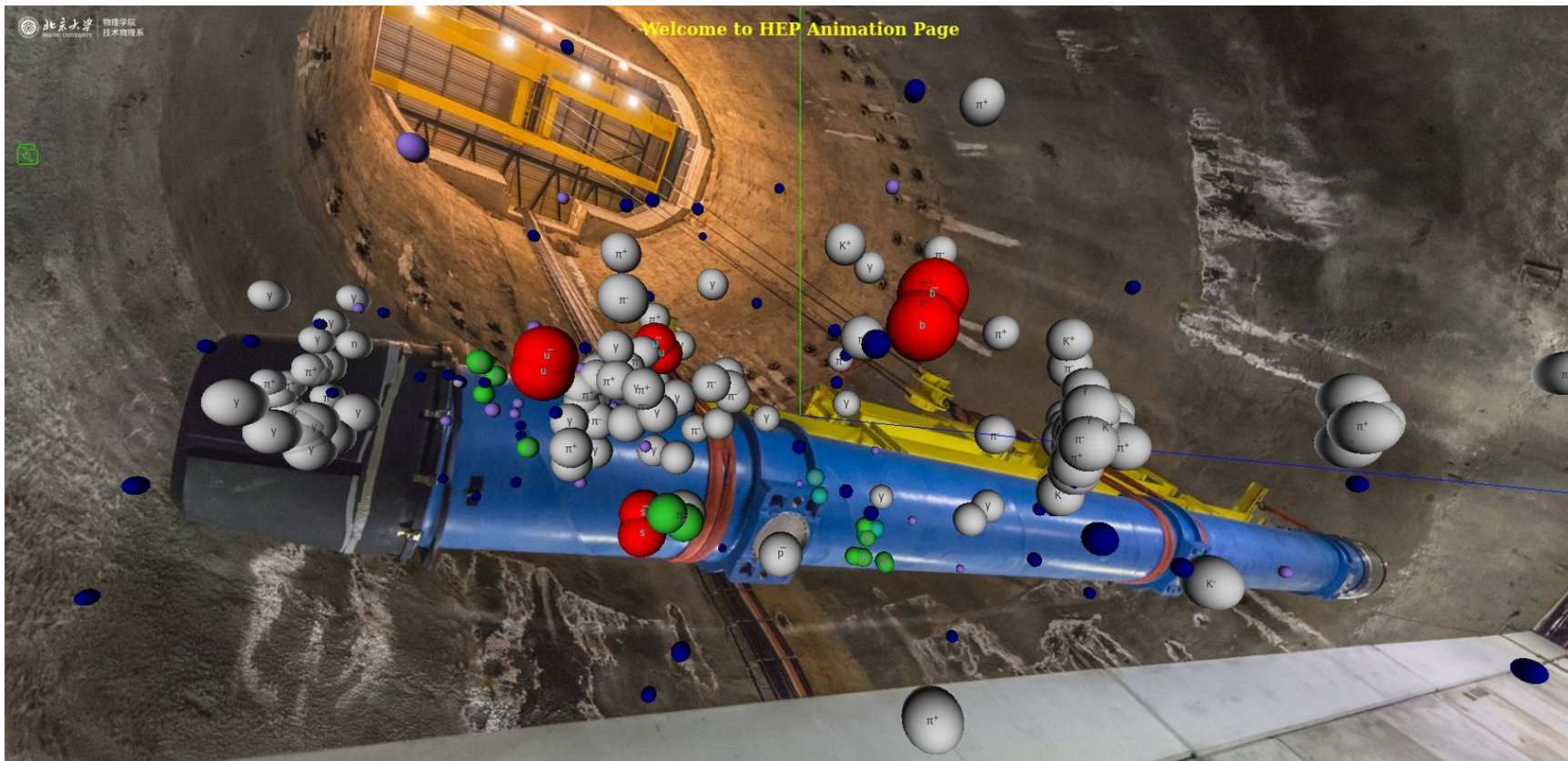
$\Delta\eta_{jj} = 5.4$

22

Backup



An animation cartoon for 4 Z boson event at the LHC



Higgs without Higgs



TABLE I. Each effect (left-hand column) can be measured as an on-shell Higgs coupling (diagram in the HC column) or in a high-energy process (diagram in the HwH column), where it grows with energy as indicated in the last column.

	HC	HwH	Growth
κ_t \mathcal{O}_{y_t}			$\sim(E^2/\Lambda^2)$
κ_λ \mathcal{O}_6			$\sim(vE/\Lambda^2)$
$\kappa_{Z\gamma}$ \mathcal{O}_{WW} $\kappa_{\gamma\gamma}$ \mathcal{O}_{BB} κ_V \mathcal{O}_r			$\sim(E^2/\Lambda^2)$
κ_g \mathcal{O}_{gg}			$\sim(E^2/\Lambda^2)$

HCs are associated with an EFT Lagrangian $\mathcal{L} = \sum_i c_i \mathcal{O}_i / \Lambda^2$, consisting in particular of the dimension-six operators [12,13],

$$\begin{aligned}
 \mathcal{O}_r &= |H|^2 \partial_\mu H^\dagger \partial^\mu H, & \mathcal{O}_{y_\psi} &= Y_\psi |H|^2 \psi_L H \psi_R, \\
 \mathcal{O}_{BB} &= g^2 |H|^2 B_{\mu\nu} B^{\mu\nu}, & \mathcal{O}_{WW} &= g^2 |H|^2 W_{\mu\nu}^a W^{a\mu\nu}, \\
 \mathcal{O}_{GG} &= g_s^2 |H|^2 G_{\mu\nu}^a G^{a\mu\nu}, & \mathcal{O}_6 &= |H|^6,
 \end{aligned} \tag{1}$$

with Y_ψ the Yukawa coupling for the fermion ψ . [Note that the parameters in Eq. (3) can be put in correspondence with other parametrizations of HCs: via partial widths $\kappa_i^2 = \Gamma_{h \rightarrow ii} / \Gamma_{h \rightarrow ii}^{\text{SM}}$ [14], via Lagrangian couplings in the unitary gauge g_{hii} [13,15], or via pseudo-observables [16].]

The operators of Eq. (1) have the form $|H|^2 \times \mathcal{O}^{\text{SM}}$, with \mathcal{O}^{SM} a dimension-four SM operator (i.e., kinetic terms, Higgs potential, and Yukawa couplings) times

The Monte Carlo (MC) simulation used for this analysis can be divided into signal and background samples. The ZZ signal production via quark-antiquark annihilation is simulated at next-to-leading order (NLO) with MadGraph5_aMC@NLO [19] and POWHEG 2.0 [20–23]. The $gg \rightarrow ZZ$ process is simulated at leading order (LO) with MCFM [24]. The cross sections of these samples are normalized to the cross sections calculated at NNLO for $q\bar{q} \rightarrow ZZ$ [15] (K factor of 1.1) and at NLO in QCD for $gg \rightarrow ZZ$ [25] (K factor of 1.7). The production via SM Higgs

boson production and decay (in particular $gg \rightarrow H \rightarrow ZZ$) is simulated with POWHEG at NLO. Electroweak ZZ production in association with two jets is simulated with MadGraph [19] at LO. The nominal SM signal predictions in this analysis are derived from the MadGraph5_aMC@NLO $q\bar{q} \rightarrow ZZ$ sample, the MCFM $gg \rightarrow ZZ$ samples, and the MadGraph EW production sample, which includes vector boson fusion (VBF) Higgs events and their interference with non-Higgs EW production, and the POWHEG $H \rightarrow ZZ$ samples.

Results in this note are also compared to the very recent nNNLO+PS predictions [26], which consist of NNLO predictions for quark-initiated channel combined with parton showers using the MiNNLO_{PS} method, and NLO predictions for loop-induced gluon fusion channel matched to parton showers, with event generators for the two channels implemented in the POWHEG framework. Spin correlations, interferences and off-shell effects are included by calculating the full process $pp \rightarrow \ell^+ \ell^- \ell'^+ \ell'^-$ and considering all contributions to the four-lepton final state.

As part of the nNNLO+PS predictions, the NNLO+PS $q\bar{q} \rightarrow ZZ$ predictions from the MiNNLO_{PS} method are NNLO accurate for inclusive production and NLO accurate for Z+1-jet production. The combination of the two jet multiplicities does not require any unphysical merging scale [27]. These predictions are expected to give better descriptions at high jet multiplicities than the POWHEG $q\bar{q} \rightarrow ZZ$ predictions, which are NLO accurate in inclusive production, and the MadGraph5_aMC@NLO predictions, which were simulated at NLO with the 0-jet and 1-jet processes, and merged using FxFx scheme [28].

data are unfolded for detector effects using the iterative D'Agostini's method [40] including correction for background contributions, with the RooUnfold toolkit as described in Ref. [41], and compared with the theoretical predictions from (MadGraph5_aMC@NLO $q\bar{q} \rightarrow ZZ$)+(MCFM $gg \rightarrow ZZ$)+(POWHEG $H \rightarrow ZZ$), and (POWHEG $q\bar{q} \rightarrow ZZ$)+(MCFM $gg \rightarrow ZZ$)+(POWHEG $H \rightarrow ZZ$), where MadGraph EW ZZ predictions are also added to these two sets of predictions. The unfolded results are also compared with the nNNLO+PS predictions. The truth-level distributions use generator-level leptons "dressed" by adding the momenta of generator-level photons within $\Delta R(\ell, \gamma) < 0.1$ from direction of the lepton.

In constructing the response matrix, there are MC events that pass the reconstruction-level selections, but do not have corresponding events at truth level that pass the fiducial selections. In the `RooUnfold` toolkit's implementation of the D'Agostini's method, these out-of-fiducial events are treated equivalently as background events that propagate from an additional truth-level bin to the reconstruction-level bins. The size of contribution of these out-of-fiducial events can be up to 15% for events with at least 1 jet. In addition, instead of subtracting the non-prompt and VVV backgrounds from data, we added these background events to the out-of-fiducial events with the mentioned treatment to avoid problem of having negative signal bin contents in regions of low data statistics.

Most systematic uncertainties are propagated through unfolding by recomputing the response matrix with the sample used in building the matrix shifted or reweighted to reflect a 1σ shift in the quantity of interest. The uncertainty related to that quantity is taken as the resulting normalized shape difference in the final unfolded distribution.

Observable	Signal Region	$t\bar{t}\gamma$ Control Region
Number of signal leptons	≥ 2 opposite sign, same flavour	≥ 2 opposite sign, different flavour
Lepton	$p_T(\ell_1) > 30$ GeV, $p_T(\ell_2) > 25$ GeV	
Photon	≥ 1 photon with $p_T^\gamma > 30$ GeV	
$m_{\ell\ell}$		> 40 GeV
$m_{\ell\ell} + m_{\ell\ell\gamma}$		> 182 GeV

Source	$ee + \mu\mu$
Z γ +jets signal	73 500 \pm 50 (stat.) \pm 2 600 (syst.)
Z + jets	9 800 \pm 460 (stat.) \pm 2 100 (syst.)
$t\bar{t}\gamma$	3 600 \pm 10 (stat.) \pm 540 (syst.)
Pile-up	2 500 \pm 70 (stat.) \pm 700 (syst.)
Multiboson	950 \pm 5 (stat.) \pm 280 (syst.)
$tW\gamma$	150 \pm 1 (stat.) \pm 45 (syst.)
Total prediction	90 500 \pm 500 (stat.) \pm 3 500 (syst.)
Data	96 410

The primary vertex position z_{vtx} has a Gaussian distribution with a measured width of $\sigma(z_{\text{vtx}}) \sim 35$ mm [14], corresponding to the width of the luminous region. The fraction f_{PU} can then be written as:

$$f_{\text{PU}} = \frac{1}{N_{\text{data}}} \cdot \frac{N_{\text{data}}^{\text{PU}} - N_{\text{MC}}^{\text{PU}}}{P_{\text{PU}}},$$

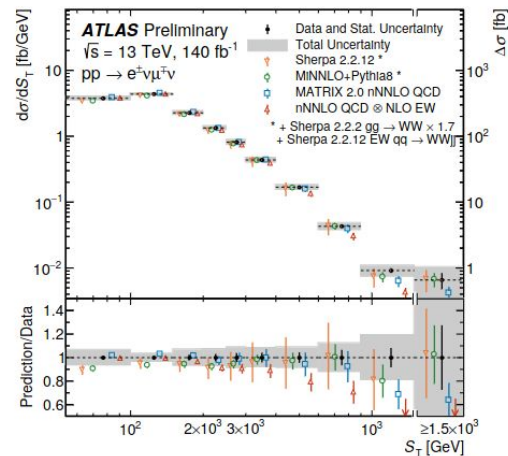
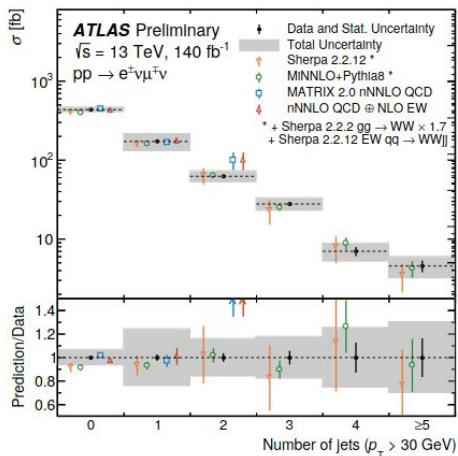
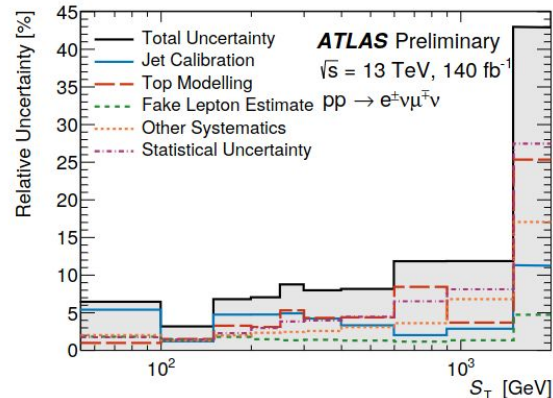
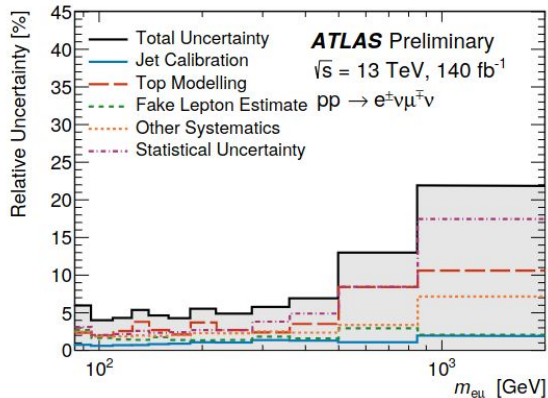
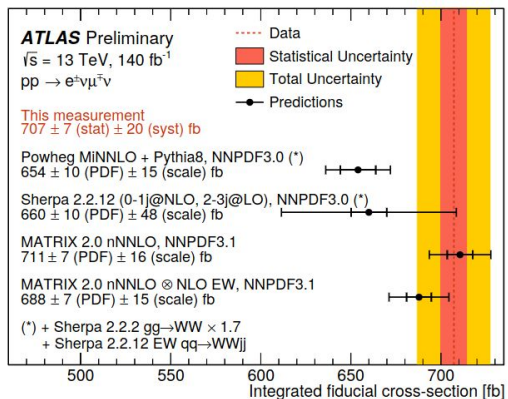
where $N_{\text{data(MC)}}^{\text{PU}}$ is the number of data (MC) events in a region dominated by pile-up, defined as the region with $|\Delta z| = |z_{\text{vtx}} - z_\gamma| > 50$ mm. Since the pile-up events are Gaussian-distributed with a width $\sigma(z_{\text{vtx}} - z_\gamma) = \sqrt{2}\sigma(z_{\text{vtx}}) \sim 50$ mm, the probability of observing events with $|\Delta z| > 50$ mm is estimated to be $P_{\text{PU}} = 0.32$. The term N_{MC} describes the MC events where the Z boson and the photon come from the same pp collision, and is taken from signal MC simulation. The MC sample is normalised to the data with $|\Delta z| < 5$ mm. The $|z_{\text{vtx}} - z_\gamma|$ distribution is shown in Figure 3 of Ref. [14]. To have a better description of the pile-up events in the differential observables, f_{PU} is computed as a function of N_{jets} and p_T^γ . The estimated f_{PU} varies from 0.02 to 0.08.

Table 4: Definition of the fiducial region at particle level.

Quantity	Selection criteria
Lepton kinematics	$p_T(\ell_1) > 30$ GeV, $p_T(\ell_2) > 25$ GeV, $ \eta < 2.47$
Photon kinematics	$p_T > 30$ GeV, $ \eta < 2.37$, $\Delta R(\gamma, \ell) > 0.4$
Photon isolation	$E_T^{\text{iso}}/E_T^\gamma < 0.07$
Jet kinematics	$(p_T > 30$ GeV if $ \eta < 2.5$) or $(p_T > 50$ GeV if $2.5 < \eta < 4.5$), $\Delta R(\gamma, \text{jet}) > 0.4$
Invariant mass	$m_{\ell\ell} > 40$ GeV, $m_{\ell\ell} + m_{\ell\ell\gamma} > 182$ GeV

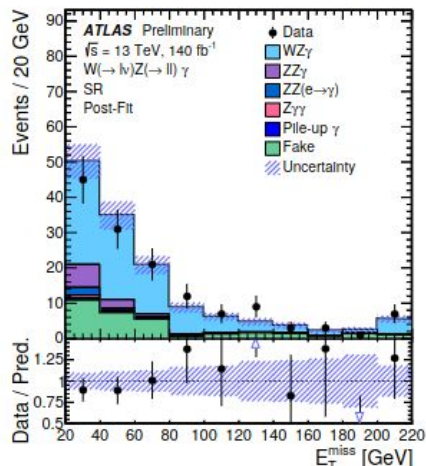
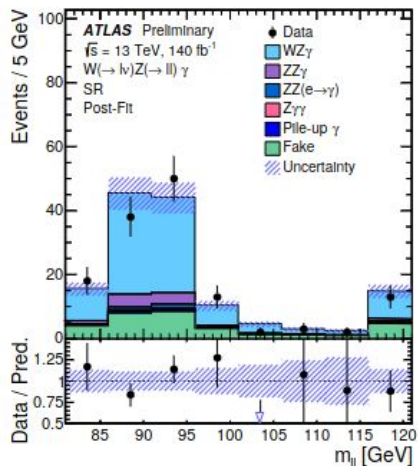
Leptons are required to pass the same p_T requirements as in the SR: $p_T(\ell_1) > 30$ GeV, $p_T(\ell_2) > 25$ GeV. However, the η requirements are different: for both electrons and muons $|\eta(\ell)| < 2.47$ is required, since at particle level the discontinuities in the detector are not present. A particle-level isolation requirement is applied to photons: the scalar sum of the E_T of all particles, except muons and neutrinos, within a cone of size $\Delta R = 0.2$ around the photon must be less than 7% of the transverse energy of the photon, E_T^γ . This selection is the same as in Ref. [14] and is optimised to achieve the same level of acceptance in both the detector-level and particle-level selections. Photons are rejected if they are within $\Delta R = 0.4$ of any lepton. Jets are obtained by clustering stable particles, excluding prompt leptons and using the anti- k_r algorithm

The differential cross-sections are determined using an iterative Bayesian unfolding method [92, 93]. In contrast to the integrated cross-section measurement, these results only weakly depend on the signal model,



$WZ\gamma, W\gamma\gamma$ observation

ATLAS-CONF-2023-014 ATLAS-CONF-2023-005

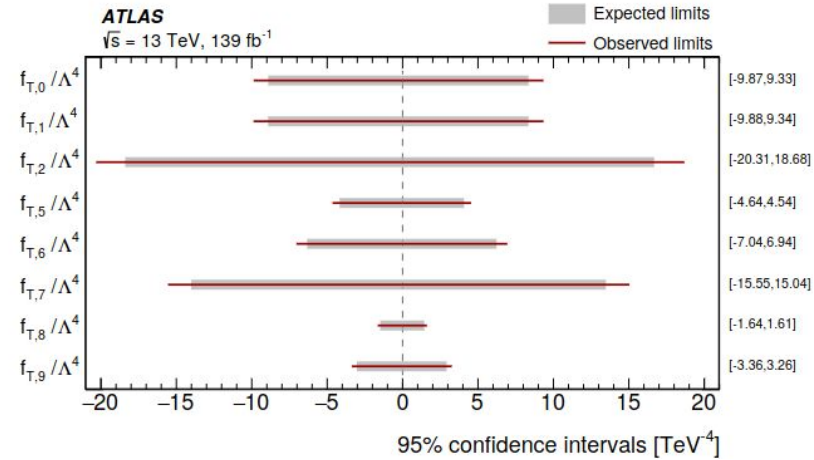
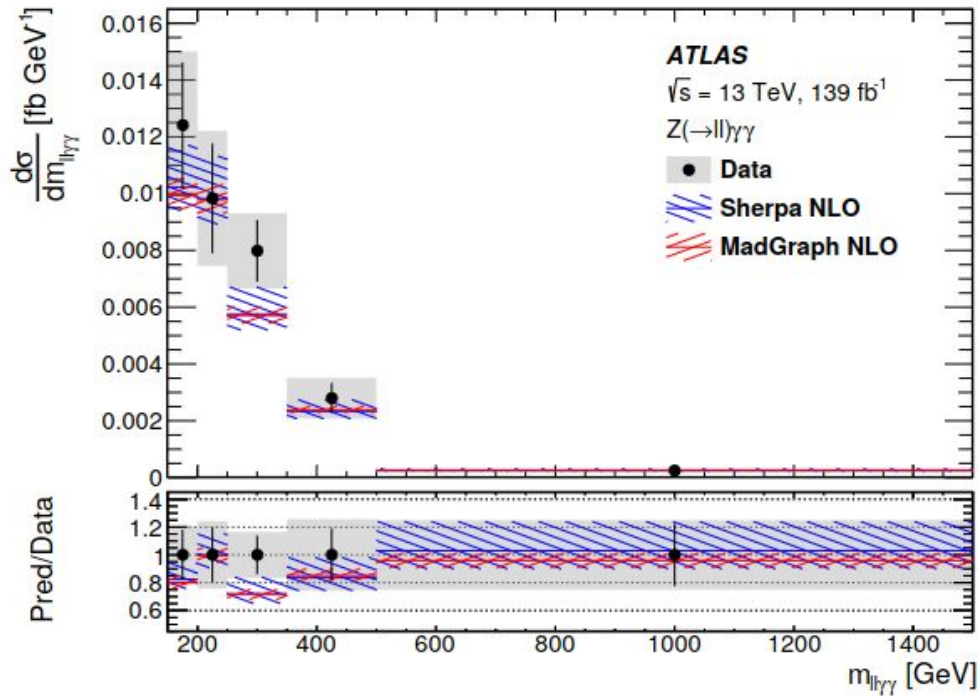


Source	SR	TopCR
$W\gamma\gamma$	410 ± 60	28 ± 5
Non-prompt $j \rightarrow \gamma$	420 ± 50	42 ± 20
Misidentified $e \rightarrow \gamma$	155 ± 11	120 ± 9
Multiboson ($WH(\gamma\gamma), WW\gamma, Z\gamma\gamma$)	76 ± 13	5.2 ± 1.7
Non-prompt $j \rightarrow \ell$	35 ± 10	–
Top ($t\ell\gamma, tW\gamma, tq\gamma$)	30 ± 7	136 ± 32
Pileup	10 ± 5	–
Total	$1\,136 \pm 34$	332 ± 18
Data	1 136	333

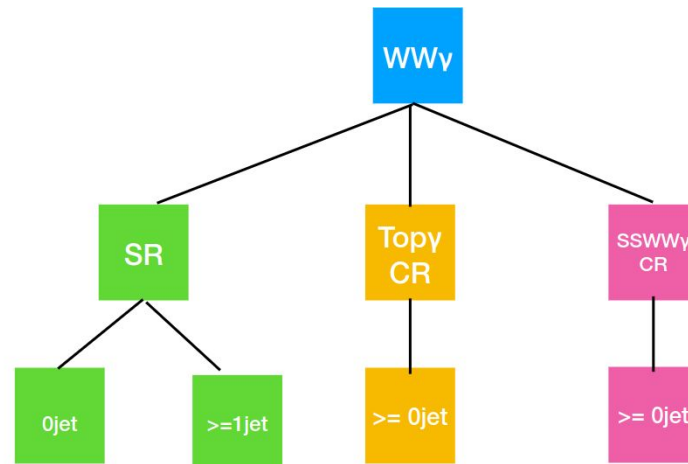
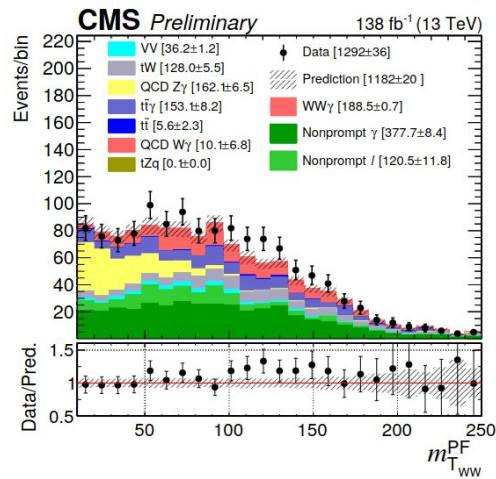
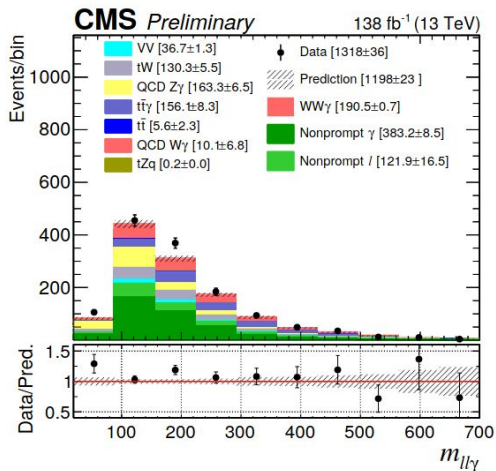
In order to obtain an unfolded production cross-section measurement, a fiducial phase space is defined to be as close as possible to the SR event sample selected at detector-level. Fiducial requirements are applied to dressed leptons, which are particle-level electrons and muons recombined with radiated photons within a cone of $\Delta R = 0.1$. Events are required to have a dressed electron or muon with $p_T > 25$ GeV and $|\eta| < 2.47$ while the two particle-level photons must satisfy $p_T > 20$ GeV, $|\eta| < 2.37$, and the isolation requirement $(E_T^{\text{cone40}} - 0.039 \times p_T) < 6.2$ GeV. Additionally, two separation requirements are applied to the two photons and between the lepton and each photon: $\Delta R_{\gamma\gamma} > 0.4$ and $\Delta R_{\ell\gamma} > 0.4$. Finally, fiducial events must satisfy $E_T^{\text{miss}} > 25$ GeV, $m_T^W > 40$ GeV, and a veto on b -jets with $p_T > 20$ GeV. Events from $W \rightarrow \tau\nu$ decays that pass these requirements are not considered as signal.

The SM predicted fiducial cross-section, $\sigma_{\text{fid}}^{\text{SM}}$, obtained using the SHERPA 2.2.11 event generator is 1.50 ± 0.01 (stat.) ± 0.02 (PDF+ α_s) ± 0.06 (scale) fb. This value does not include the effect of NLO EW corrections which have been found to be $k_{\text{EW}} = \sigma_{\text{fid}}^{\text{NLO EW}} / \sigma_{\text{fid}}^{\text{LO}} = 1.05$ [36] for the subprocess $pp \rightarrow WZ\gamma \rightarrow e^+ \nu_e \mu^+ \mu^- \gamma$. The measured cross section in the FR is $\sigma_{WZ\gamma} = 2.01 \pm 0.30$ (stat.) ± 0.16 (syst.) fb, which is consistent with the SM prediction within 1.5 standard deviations.

NLO electroweak and QCD corrections to the production of a photon with three charged lepton plus missing energy at the LHC



WW γ observation *CMS-PAS-SMP-22-006*



m_T^{WW}	[10,40,70,110,∞]	[10,40,70,110,∞]	[10,∞]	[10,40,70,110,∞]
$m_{ll\gamma}$	[20,150,250,∞]	[20,150,250,∞]	[20,∞]	[20,∞]

■ Perform simultaneous fit for events

■ Using the 2D variable (m_T^{WW} and $m_{ll\gamma}$) to build the likelihood function for SR

Flat Direction scenario:

production and decay rates at the LHC [57–59] (see also Ref. [14]), unless further assumptions are made. The effect of an enhanced Higgs Yukawa coupling y_q to a light quark $q = u, d, c, s$ on the Higgs branching fractions may be compensated by a related increase of the Higgs couplings to gauge bosons and third-generation fermions, leading to a “flat direction” in the fit along which the Higgs signal strengths remain unchanged. From the present good agreement between SM predictions and LHC Higgs measurements [22,60,61], this flat direction may be approximately described by a single generic κ_h enhancement factor for all Higgs couplings other than the light quark Yukawa y_q of interest [14]:

$$\kappa_h^2 \simeq \frac{1 - Br_{q\bar{q}}^{\text{SM}}}{2} + \frac{\sqrt{(1 - Br_{q\bar{q}}^{\text{SM}})^2 + 4Br_{q\bar{q}}^{\text{SM}}\kappa_q^2}}{2}, \quad (4)$$

with $Br_{q\bar{q}}^{\text{SM}}$ being the branching fraction for $h \rightarrow q\bar{q}$ in the SM. While the combination of Higgs signal strengths with other measurements—e.g., with electroweak precision observables or an indirect measurement of the Higgs total width (model-dependent, see Ref. [62])—can help in lifting the flat direction [Eq. (4)], this discussion highlights the importance of complementary probes of Higgs couplings to light quarks.

https://twiki.cern.ch/twiki/bin/view/LHCPhysics/LHCHWG2KAPPA?redirectedfrom=LHCPhysics.LHCHXSWG2KAPPA#1_gluon_gluon_Fusion_Process

$$\kappa_g^2 = 1.042\kappa_t^2 + 0.002\kappa_b^2 - 0.040\kappa_t\kappa_b - 0.005\kappa_t\kappa_c + 0.0005\kappa_b\kappa_c + 0.00002\kappa_c^2$$

Probing the Higgs–strange-quark coupling at e^+e^- colliders using light-jet flavor tagging

J. Duarte-Campderros,^{1,2,*} G. Perez,^{3,†} M. Schlaffer^{3,‡}, and A. Soffer^{4,§}


¹Universidad de Cantabria Instituto de Física de Cantabria (IFCA),
Avda. Los Castros s/n, E-39005 Santander, Spain

²European Organization for Nuclear Research (CERN),
EP-CMX Department CH-1211 Geneva 23, Switzerland

³Department of Particle Physics and Astrophysics, Weizmann Institute of Science, Rehovot 7610001, Israel

⁴School of Physics and Astronomy, Tel-Aviv University, Tel-Aviv 69978, Israel

- [11] M. Aaboud *et al.* (ATLAS Collaboration), *Phys. Rev. Lett.* **119**, 051802 (2017).
- [12] V. Khachatryan *et al.* (CMS Collaboration), *Phys. Lett. B* **744**, 184 (2015).
- [13] G. Perez, Y. Soreq, E. Stamou, and K. Tobioka, *Phys. Rev. D* **92**, 033016 (2015).
- [14] M. Aaboud *et al.* (ATLAS Collaboration), *J. High Energy Phys.* **07** (2018) 127.

 (Received 29 April 2019; revised manuscript)

However, it is important to note that the flavor puzzle is related to the mass hierarchy among all three generations of up-type quarks (u , c , t), down-type quarks (d , s , b), and charged leptons (e , μ , τ). Therefore, direct measurements of the smaller couplings of the Higgs to the first two generations of the different sectors are also necessary. So far, only upper bounds on the corresponding signal strengths have been obtained [11–14],

$$\begin{aligned} \mu_{\mu\mu} &\lesssim 2.8, & \mu_{ee} &\lesssim 3.7 \times 10^5, \\ \mu_{cc} &\lesssim 110, & \mu_{ss} &\lesssim 7.2 \times 10^8. \end{aligned} \quad (3)$$

Same-Sign WW

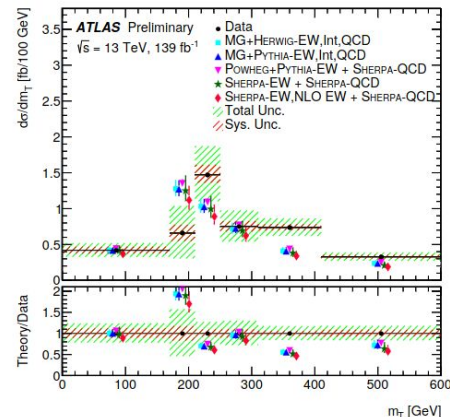
ATLAS-CONF-2023-023



Process, short description	ME Generator + parton shower	Order	Tune	PDF set in ME
EW, Int, QCD $W^\pm W^\pm jj$, nominal signal	MADGRAPH5_AMC@NLO2.6.7 + HERWIG7.2	LO	default	NNPDF3.0NLO
EW, Int, QCD $W^\pm W^\pm jj$, alternative shower	MADGRAPH5_AMC@NLO2.6.7 + PYTHIA8.244	LO	A14	NNPDF3.0NLO
EW $W^\pm W^\pm jj$, NLO pQCD approx.	SHERPA2.2.11 ²	+0,1j@LO	Sherpa	NNPDF3.0NNLO
EW $W^\pm W^\pm jj$, NLO pQCD approx.	POWHEG Boxv2 + PYTHIA8.230	NLO (VBS approx.)	AZNLO	NNPDF3.0NLO
QCD $W^\pm W^\pm jj$, NLO pQCD approx.	SHERPA2.2.2	+0,1j@LO	Sherpa	NNPDF3.0NNLO
QCD $VVjj$	SHERPA2.2.2	+0,1j@NLO; +2,3j@LO	Sherpa	NNPDF3.0NNLO
EW $W^\pm Zjj$	MADGRAPH5_AMC@NLO2.6.2+PYTHIA8.235	LO	A14	NNPDF3.0NLO
EW $ZZjj$	SHERPA2.2.2	LO	Sherpa	NNPDF3.0NNLO
QCD $V\gamma jj$	SHERPA2.2.11	+0,1j@NLO; +2,3j@LO	A14	NNPDF3.0NNLO
EW $V\gamma jj$	MADGRAPH5_AMC@NLO2.6.5+PYTHIA8.240	LO	A14	NNPDF3.0NLO
VVV	SHERPA2.2.1 (leptonic) & SHERPA2.2.2 (one $V \rightarrow jj$)	+0,1j@LO	Sherpa	NNPDF3.0NNLO
$t\bar{t}V$	MADGRAPH5_AMC@NLO2.3.3.p0 + PYTHIA8.210	NLO	A14	NNPDF3.0NLO

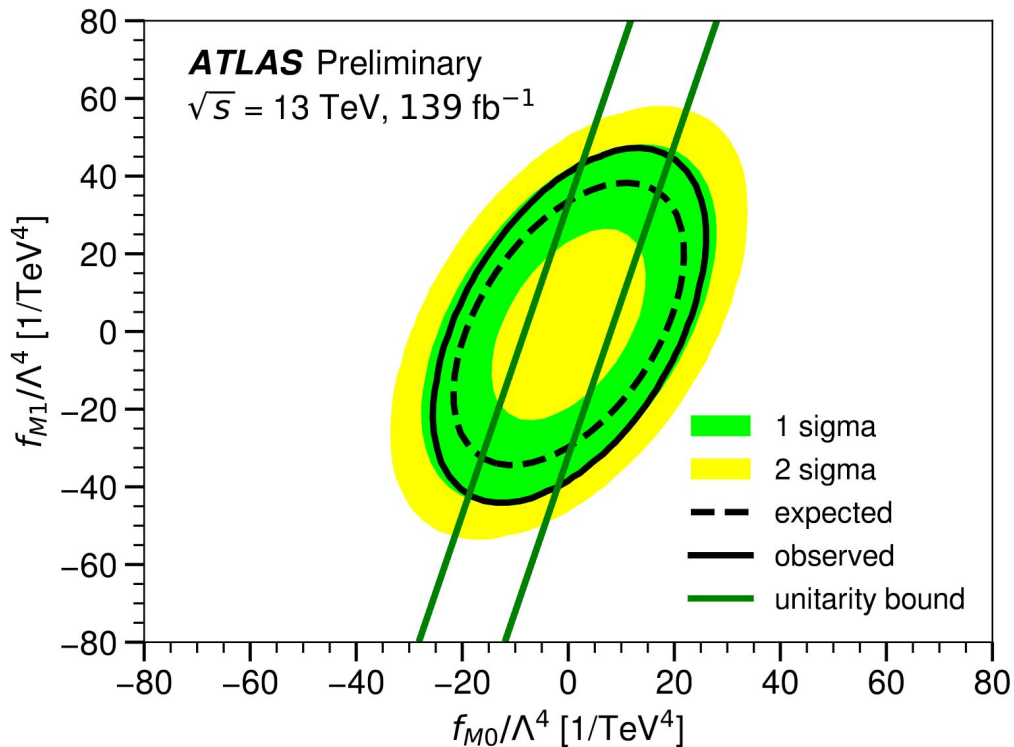
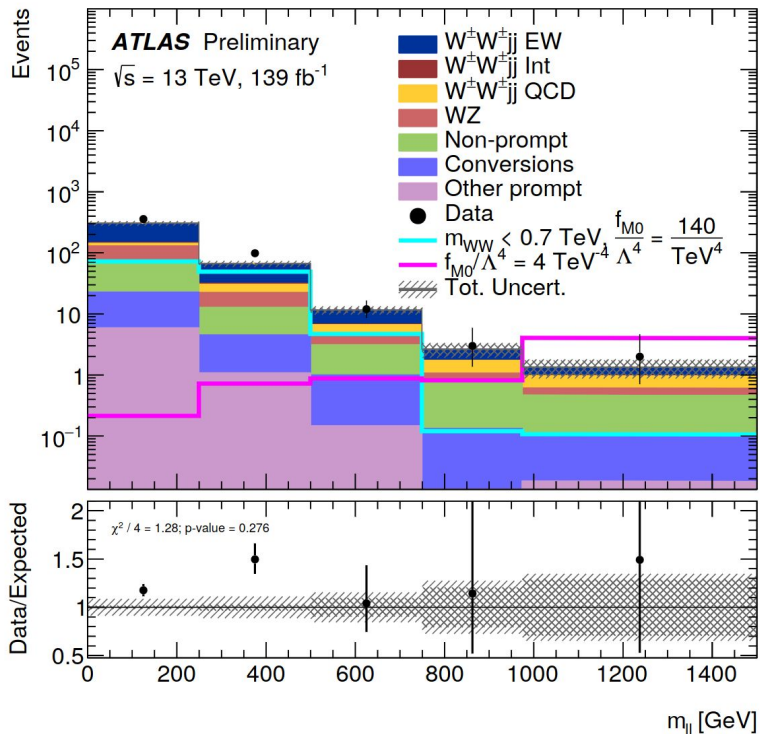
MG+Herwig

Variable	EW $W^\pm W^\pm jj$		Inclusive $W^\pm W^\pm jj$	
	χ^2/N_{dof}	p -value	χ^2/N_{dof}	p -value
$m_{\ell\ell}$	4.4/6	0.623	7.0/6	0.322
m_T	12.9/6	0.045	15.9/6	0.014
m_{jj}	7.2/6	0.300	7.8/6	0.250
$N_{\text{gap jets}}$	2.3/2	0.316	2.3/2	0.316
ξ_{J3}	4.3/5	0.511	5.2/5	0.396



Same-Sign WW

ATLAS-COM-CONF-2023-031 [EpJ C 81 \(2021\) 723](#)



$ZZ \rightarrow 4l + \text{jets}$

ATLAS-COM-CONF-2023-032

Source	Uncertainty (%)
Luminosity	0.8 – 1.3
Leptons	0.8 – 1.6
Jets	2.7 – 18
Pile-up	0.0 – 2.5
Backgrounds	0.9 – 9.0
Theory modelling	0.6 – 8.8
Unfolding method	0.9 – 12
Total systematic	5 – 22

Wilson coefficient	$ \mathcal{M}_{d6} ^2$ Included	95% confidence interval [TeV^{-2}]	
		Expected	Observed
c_W/Λ^2	yes	[-1.3, 1.3]	[-1.2, 1.2]
	no	[-32, 32]	[-37, 28]
$c_{\widetilde{W}}/\Lambda^2$	yes	[-1.3, 1.3]	[-1.2, 1.2]
	no	[-17, 17]*	[0, 30]*
c_{HWB}/Λ^2	yes	[-16, 7]	[-16, 6]
	no	[-12, 12]	[-15, 10]
$c_{H\widetilde{W}B}/\Lambda^2$	yes	[-1.3, 1.3]	[-1.2, 1.2]
	no	[-67, 67]*	[-25, 130]*
c_{HB}/Λ^2	yes	[-13, 13]	[-12, 12]
	no	[-38, 38]	[-38, 38]
$c_{H\widetilde{B}}/\Lambda^2$	yes	[-13, 13]	[-12, 12]
	no	[-420, 420]*	[-200, 790]*

